

GREEN SYNTHESIS OF ZERO VALENT IRON NANOPARTICLES USING
MALVA EXTRACT AND THEIR ANTIMICROBIAL ACTIVITY

A Thesis
presented to
the Faculty of Natural and Applied Sciences
at Notre Dame University-Louaize

In Partial Fulfillment
of the Requirements for the Degree
Master of Science

by
RITA ROBERT KOLIANA

MAY 2022

© COPYRIGHT

By

Rita Koliana

2022

All Rights Reserved

Notre Dame University – Louaize

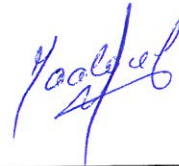
Faculty of Natural and Applied Sciences

Department of Sciences

We hereby approve the thesis of

Rita Koliانا

Candidate for the degree of Science in Industrial Chemistry



Dr. Rita Maalouf

Supervisor, Chair



Dr. Kamil Rahme

Committee Member



Dr. Layla Badr

Committee Member

Acknowledgements

I would like first to thank my thesis advisor Dr. Rita Maalouf Associate Professor at the Department of Sciences – Faculty of Natural and Applied Sciences at Notre Dame University-Louaize. Dr. Maalouf was always encouraging and supportive and always steered me in the right direction while always allowing this Thesis to be my own work.

I would like to thank the committee Members, Dr Kamil Rahme and Dr Layla Badr, for accepting to review my thesis and providing me with their valuable comments

A debt of gratitude is also owed to my colleagues Melissa Maroun and Alice Kettaneh both microbiologists for assisting me during the performance of the antibacterial activity.

Finally, I cannot but express my sincere gratitude to my family and friends who provided me with unfailing support throughout my studies and research. This accomplishment would not have been possible without them.

Thank you.

Table of Contents

List of Figures	5
List of Tables	6
List of Abbreviations	7
Abstract	8
Chapter 1: Literature review	9
1.1 Nanotechnology and nanomaterials	9
1.2 Nanoparticles	11
1.3 Types and Classifications	12
1.4 Physical and Chemical properties	14
1.5 Synthesis routes of NPs	15
1.5.1 Synthetic routes of Inorganic NPs	16
1.6 Green Chemistry	18
1.6.1 Green chemistry in the synthesis of NPs	19
1.6.2 Plant mediated synthesis of nanoparticles.	20
1.7 Zero-valent Iron nanoparticles	23
1.7.1 Green synthesis of ZVI NPs	25
1.7.2 Applications of ZVI NPs	25
1.7.3 Green synthesis of iron NPs using Malva extracts	27
Chapter 2- Materials and Methods.....	29
2.1 Chemical reagents	29
2.2 Malva extract preparation	29
2.3 Synthesis of Zero valent iron nanoparticles.....	29
2.4 Characterization of the synthesized nanoparticles.....	30
2.5 Antimicrobial properties	34
Chapter 3: Results and Discussion.....	36
3.1 Effect of Malva soaking time at different pH values on the hydrodynamic size of the synthesized M-ZVI nanoparticles	36
3.2 Effect of FeCl ₃ concentration on the hydrodynamic size of the synthesized M-ZVI nanoparticles	39

3.3 Effect of pH on the hydrodynamic size and zeta potential of the synthesized M-ZVI nanoparticles.	40
3.4 FTIR Characterization	42
3.5 XRD characterization.....	44
3.6 Scanning electron microscopy Characterization.....	34
3.7 Antimicrobial activity	45
3.7 Conclusion	47
References.....	48

List of Figures

Figure 1: nanomaterial classification based on dimensions [2]	11
Figure 2: Different synthesis routes available for the synthesis of metal nanoparticles [18] ..	16
Figure 3: proposed mechanism for the formation of nanoparticles by microemulsion [20] ...	17
Figure 4: Flavonoids and their basic structure [36]	21
Figure 5: Phenolic acid and their structure [38].....	22
Figure 6: Tannins and their structure [35]	23
Figure 7: Malva Parviflora.....	28
Figure 8: A- experimental setup B-black precipitate formation	30
Figure 9 Basic DLS setup [64].....	32
Figure 10: FTIR layout [68].....	33
Figure 11: FeNPs size variation as a function of pH for different malva soaking time	37
Figure 12: size variation of FeNPs with pH for 3 different FeCl ₃ solution concentrations.....	39
Figure 13: FTIR spectrum of malva and synthesized zero valent iron nanoparticles.....	43
Figure 14: X-ray powder diffraction pattern of the synthesized zero valent iron nanoparticles	44
Figure 15: XRD spectrum of green synthesized FeNPs from leaves of <i>U. dioica</i> [70].....	45
Figure 16: SEM image of green synthesized zero valent iron nanoparticles using ricinus communis seeds extract [86].....	34
Figure 17: Positive control on E.coli and S.aureus	46
Figure 18: antibacterial activity of malva extract, FeCl ₃ and FeNPs on E.coli and S.aureus..	46

List of Tables

Table 1: Nanomaterials classification based on material.....	10
Table 2: FeNPs size variation at different pH with different malva soaking time	36
Table 3: Most favorable extraction time for studied leaves.....	38
Table 4: FeNPs size, PDI and zeta potential variation as a function of pH.....	41

List of Abbreviations

NPs	Nanoparticles
LSPR	Localized Surface Plasmon Resonance
SEM	Scanning Electron Microscopy
XRD	X-ray diffraction
FTIR	Fourier Transform Infrared Spectrometer
DLS	Dynamic Light Scattering
UV	Ultraviolet–visible spectroscopy
Fe ⁰	Zero valent Iron
FeNPs	Zero valent Iron nanoparticles
PdI	Polydispersity index
nZVI	Nanoscale zero valent Iron
M-ZVI nps	Malva- Zerovalent Iron nanoparticles

Abstract

Green synthesis of metallic nanoparticles has accumulated an ultimate interest over the last decade due to their distinctive properties that make them applicable in various fields of science and technology. Metal nanoparticles that are synthesized by using plants have emerged as nontoxic and ecofriendly. In the current study, the optimal reaction condition for the synthesis of zero valent iron nanoparticles using Malva extract was developed. For the first time, aqueous extract of Malva parviflora was used as a sustainable source of reducing and capping agents to synthesize zero valent iron nanoparticles. The resulting particles were characterized using Fourier transform infrared (FTIR) spectroscopy, X-ray diffractometer (XRD) and Malvern Zetasizer Nano ZSP-dynamic light scattering – (DLS) for size and zeta potential determination. After reaction optimization the synthesized particles at pH=7 had an average size of 130 nm with a PDI = 0.25 thus the particles can be considered as monodispersed. The prepared particles were found to be amorphous zero-valent iron nanoparticles. The FTIR showed that polyphenols which serve as reducing and stabilizing agents play a significant role in the synthesis of NPs and reduce the possibility of aggregation of NPs. Synthesized particles were tested for antimicrobial activity against human pathogenic Gram- negative Escherichia coli and Gram-positive Staphylococcus aureus. Synthesized particles were found effective against Staphylococcus aureus while ineffective against Escherichia coli.

Keywords: Green synthesis, Malva parviflora, Zero valent iron nanoparticles, antimicrobial activity.

Chapter 1: Literature review

1.1 Nanotechnology and nanomaterials

Nanotechnology is a rapidly growing field that deals with designing, characterizing, producing, and manipulating of materials, structures and devices having one or more dimensions of the order of 100 nm or less. The concept of nanotechnology was introduced by Richard Feynman in 1959 in his talk “There's Plenty of Room at the Bottom”, in which he defined the possibility of synthesis via direct manipulation of atoms. Since then, the progress in nanotechnology has sparked a science revolution in many fields: information technology, homeland security, medicine, transportation, energy, food safety, and environmental science, among many others. Nanotechnology is one of the most promising technologies of the 21st century [1].

Nanomaterials are one of the main products of nanotechnology. They are classified into different categories based on the materials used in the synthesis process and the number of dimensions.

Four classifications can be adopted based on materials: [2]

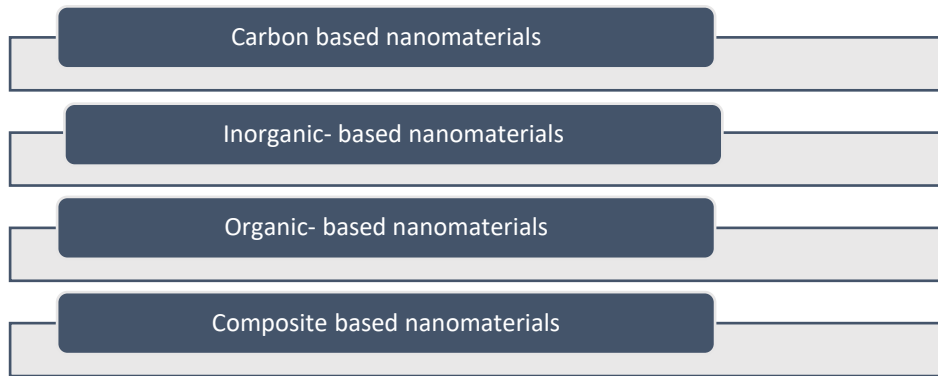


Table 1: Nanomaterials classification based on material

1. Carbon-based nanomaterials: This type of nanomaterials is composed of carbon and can have various morphologies. The carbon-based nanomaterials can be hollow tubes or spheres, carbon nanofibers, Fullerenes, and graphene [2].
2. Inorganic-based nanomaterials: This type of nanomaterials is made up of metals and metal oxides. They can be produced from metals such as Ag, Au, and Fe or from metal oxides such as TiO₂, ZnO, and MnO₂. Semiconductor nanomaterials are also synthesized from silicon and ceramic materials.
3. Organic-based nanomaterials: This type of nanomaterials is made up of organic matter other than carbon and inorganic material.
4. Composite based nanomaterials: Composite nanomaterials are made up of one or more layer of nanoparticles. These nanomaterials are combined with other nanoparticles, bulk materials, or more complex materials like metal frameworks.

Four classifications can be adopted based on the dimension: [3]

1. Zero-dimensional nanomaterials: It's the most common type of nanomaterials with dimensions within the nanoscale range. No dimension is greater than 100 nm. It includes quantum dots, nanospheres and nanoclusters.

2. One-dimensional nanomaterials: In this type, one of the dimensions is greater than 100 nm while the other dimensions are within the nanoscale. The most common examples are nanotubes, nanowires and nanorods.
3. Two-dimensional nanomaterials: This type of nanomaterials has a plate like structure where two dimensions are greater than 100 nm. The most common examples are the nanofilms and nanolayers.
4. Three-dimensional nanomaterials: This type of nanomaterials is not confined to the nanoscale in any dimension. Nano range particles come together to form three-dimensional nanomaterials such as nanocomposites, bundles of nanofibers, and multilayer type structures.

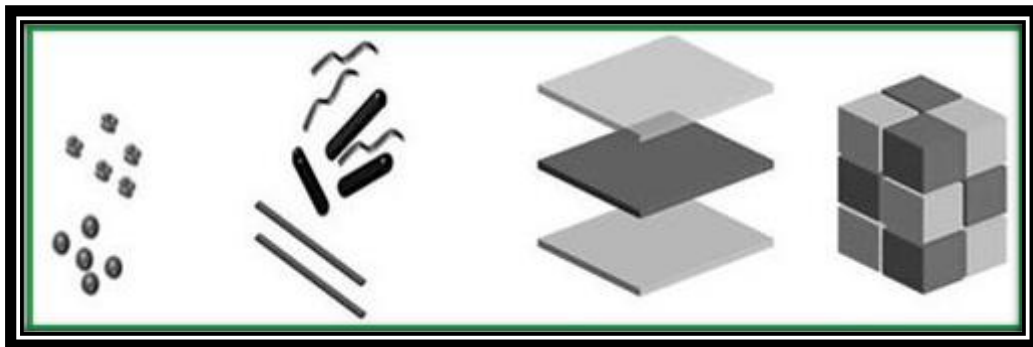


Figure 1: nanomaterial classification based on dimensions [2]

1.2 Nanoparticles

Nanoparticles (NPs) play a major role in nanotechnology and find use in many applications. The prefix *Nano* has its origin in the Greek and Roman terms “Nannos/Nanus”, which describe dwarfs or dwarf-like stages of living organisms. The discovery, enhancement and use of light microscopes opened insights in the world of miniscule structures, which were later enormously deepened by the new microscopical technologies [4]. These technologies

made it possible to discover, to define and to use a wide range of new structures of only few nanometers in size, which at first were named as “Ultra fine Particles” [5]. Soon afterwards, these ultrafine particles were named “Nanoparticles”. Their size range between 1 and 100 nm, whereby 1 nm is 1×10^{-9} m [6].

1.3 Types and Classifications

NPs are broadly divided into various categories depending on their morphology, size, physical and chemical properties. They are commonly divided into two main groups: organic and inorganic. They can also be classified according to their physical and chemical properties as follows:

- i. Carbon-based NPs: Generally, these NPs contain carbon, and are found in morphologies such as hollow tubes, ellipsoids or spheres. They gained interest due to their electrical conductivity, high strength, structure, electron affinity, and versatility. Due to their properties, they are used as fillers, efficient gas adsorbents for environmental remediation and as support medium for different inorganic and organic catalysts [7].
- ii. Ceramics NPs: These are inorganic nonmetallic solids synthesized via heat and successive cooling. They can be found in amorphous, polycrystalline, dense, porous or hollow forms. Therefore, these NPs are getting great attention of researchers due to their use in applications such as catalysis [8].
- iii. Semiconductor NPs: Semiconductor materials own properties between metals and nonmetals. Semiconductor NPs possess wide bandgaps and therefore show significant

alteration in their properties with bandgap tuning. Therefore, they are very important materials in photocatalysis, photo optics and electronic devices [9].

- iv. Polymeric NPs also called organic-based NPs: These include NPs made from organic matter excluding carbon-based or inorganic-based NPs. The utilization of noncovalent interactions for the self-assembly helps to transform the organic NPs into desired structures such as dendrimers, liposomes and polymer NPs.
- v. Lipid-based NPs: These NPs contain lipid moieties and are effectively used in many biomedical applications. Lipid NPs possess a solid core made of lipid and a matrix contains soluble lipophilic molecules. Surfactants or emulsifiers stabilize the external core of these NPs [10].
- vi. Metallic NPs also called inorganic-based NPs: These NPs include metal and metal oxide, they can be synthesized into metals such Au or Ag, metal oxides such as TiO_2 and ZnO, and semiconductors such as silicon. These NPs possess unique optoelectrical properties. Due to their properties, metal NPs find applications in many research areas [7]. This type of NPs will be our focus in this work.

In the field of nanotechnology, metallic nanoparticles have shown number of properties that have opened many new paths in nanotechnology. In 1857, Faraday was the first to recognize the presence of metallic nanoparticles in a solution. Metallic nanoparticles have physical and chemical properties such as mechanical strength, high surface area, low melting point, optical properties and magnetic properties different from their bulk metals [11, 12]. Metal nanoparticles are made of pure metals: Gold, Platinum, Silver, Iron, Titanium, or their compounds: oxides, hydroxides, sulfides, phosphates, fluorides, and chlorides.

Due to well-known localized surface Plasmon resonance characteristics, these NPs possess unique optical and electrical properties [7]. LSPR is an optical phenomenon generated by a light wave trapped within conductive nanoparticles smaller than the wavelength of light [13]. The phenomenon is a result of the interactions between the incident light and surface electrons in a conduction band. This interaction produces coherent localized Plasmon oscillations with a resonant frequency that strongly depends on the composition, size, geometry, dielectric environment, and particle–particle separation distance of NPs [14].

Any nanoparticle will have an exceptionally high surface area to volume ratio; this is one of the reasons for some of their unusual properties. However, this high surface area also means that the surface of any given nanoparticle is an important component of the material.

1.4 Physical and Chemical properties

Nanoparticles often have unique physical and chemical properties. While bulk materials have constant physical and chemical properties regardless of size, the size of a nanoparticle dictates its physical and chemical properties. Thus, the properties of a material change as its size approaches nanoscale proportions and as the percentage of atoms at the surface of a material becomes significant. Following are few physical and chemical properties that are dealt with nanostructures: [15]

i. Physical properties:

The principal physical properties of nanoparticles are described in terms of shape, size distribution, surface morphology, melting point and most importantly the optical, mechanical, magnetic, and electric properties. The mechanical strength is found to increase with decrease in the size and have a huge effect on the hardness and plasticity of the nanomaterial. The optical

properties of nanoparticles are size dependent and represent a strong UV–visible extinction band. The magnetic and electrical properties are expressed by means of conductivity, semiconductivity, and resistivity [15, 16].

ii. Chemical properties:

The reduction in particle size affects the interaction of particle in chemical reactions. When size of the particle decreases, a greater number of bonds is exposed to the environment involved in the chemical reactions/processes. Chemical properties are described in terms of surface energy, oxidation process at the nanoscale which is not observed at low temperature and the catalysis process [15].

1.5 Synthesis routes of NPs

Two approaches have been developed describing the different possibilities for the synthesis of nanostructures. These manufacturing approaches fall under two categories: top-down and bottom-up, which differ in degrees of quality, speed and cost. Briefly, in the top-down approach, nanoparticles are produced by size reduction of bulk material by lithographic techniques and by mechanical techniques such as ablation and grinding, etc., while, in bottom-up approach, small building blocks are assembled into a larger structure, e.g., chemical synthesis. However, the most acceptable and effective approach for nanoparticle preparation is the bottom-up approach, where a nanoparticle is “grown” from simpler molecules known as reaction precursors. In this way, it is likely possible to control the size and shape of the nanoparticle depending on the subsequent application through variation in precursor concentrations and reaction conditions such as temperature and pH [17].

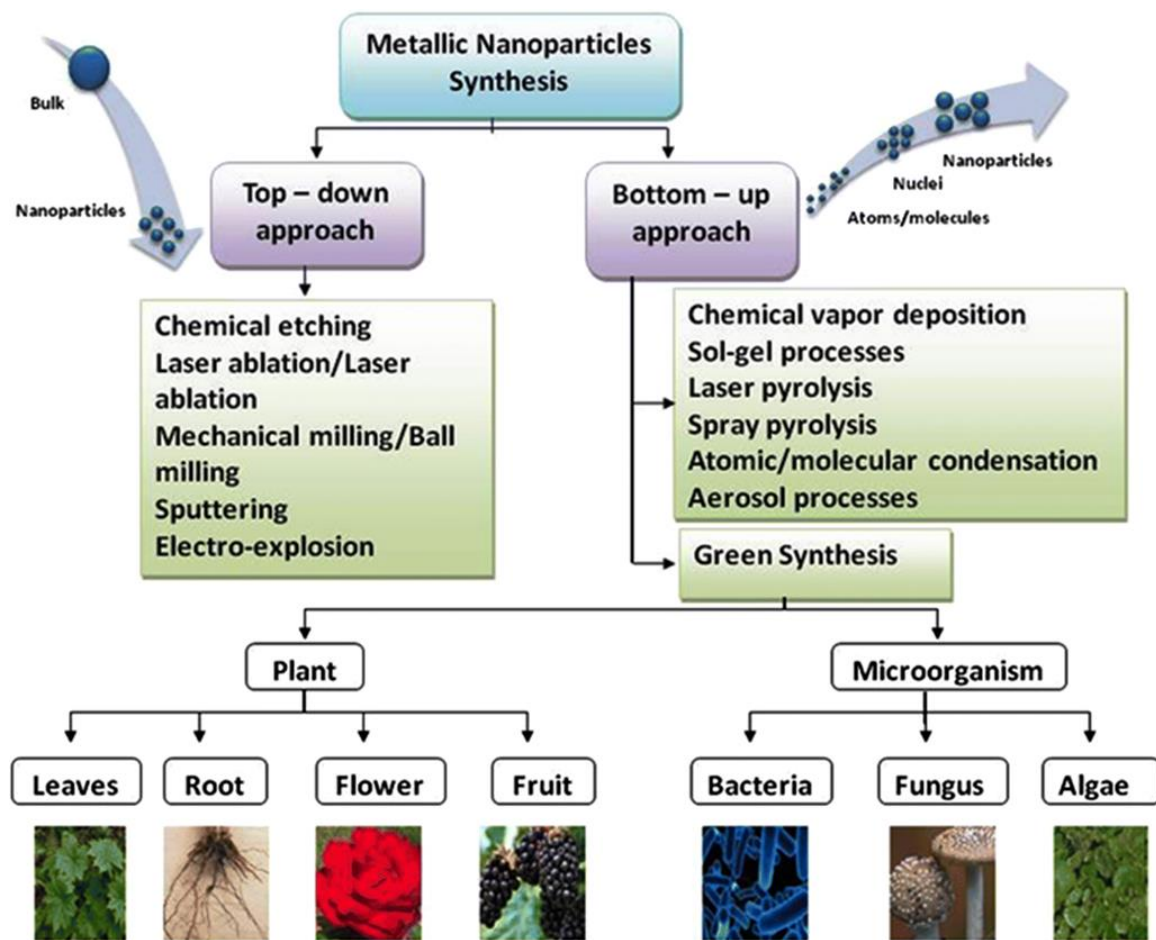


Figure 2: Different synthesis routes available for the synthesis of metal nanoparticles [18]

Synthetic routes of Inorganic NPs

Chemical methods have been very useful in the generation of NPs of various inorganic materials. As we are interested in the synthesis of zero-valent iron nanoparticles, we have detailed in this section some synthetic methods for the synthesis of inorganic NPs: [19]

1. Use of micro emulsions: This method consists of a ternary mixture of water, a surfactant or a mixture of surface-active agents and oil. This process has been used for the synthesis of various NPs by mixing two micro-emulsions containing appropriate reactants.

The mechanism of formation is given in the figure 3.

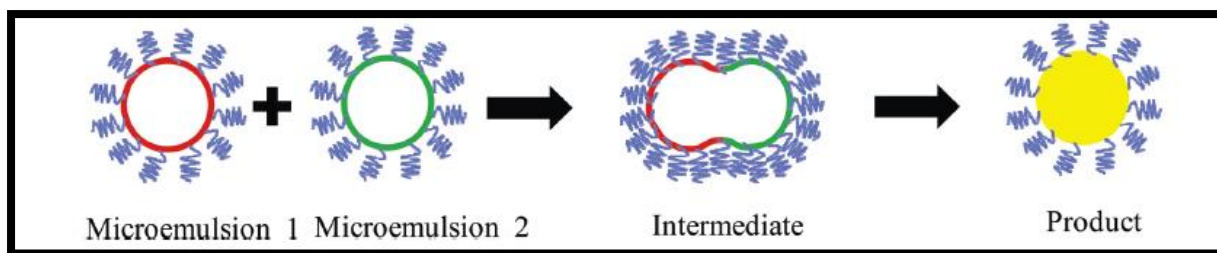


Figure 3: proposed mechanism for the formation of nanoparticles by microemulsion [20]

2. Thermal decomposition: Metal NPs are generated by the thermal decomposition of molecules containing zero-valent metals such as metal carbonyls.
3. Hydrothermal and solvothermal synthesis: Taking advantage of the high reactivity of metal salts and complexes at elevated temperatures and pressures, inorganic nanomaterials are conveniently prepared at temperatures considerably lower than in solid-state reactions. Reaction parameters such as time, temperature, pressure, reactant concentration, pH, reaction cell fill volume can be tuned to attain satisfactory nucleation rates and particle size distribution.
4. Sol-gel Method: It is generally employed for the synthesis of metal oxide NPs as well as oxide nanocomposites. It involves the hydrolysis and condensation of metal precursors. The sol-gel process can be conducted either in aqueous or non-aqueous medium.

One of the main methods used for the synthesis of iron nanoparticles is the reduction of iron salts and oxides. Reduction of salts is generally performed using familiar wet-chemical methods in the presence of a surfactant that prevents the agglomeration of the insoluble metal. Unlike the iron salts, iron oxides are soluble in strong acids or bases where iron can't be directly reduced to its zero valent state. Thus, the reduction of iron oxides to iron nanoparticles begins with the formation of iron oxide nanoparticles [21].

There are many other methods employed for the synthesis of inorganic NPs. Some of these are: photochemical synthesis, microwave method, phase transfer synthesis, use of the liquid – liquid interface, use of ionic liquids, and electrochemical synthesis. Also, biological approaches using plant and microbial sources have attracted significant interest in recent years.

1.6 Green Chemistry

Recent advances in nanoscience and nanotechnology have also led to the development of novel nanomaterials, which ultimately increase potential health and environmental hazards. Many multinational organizations including, among others, the United Nations, the European Union, and the Asian Pacific Economic Community, are now beginning to assess the role that they can play in promoting the implementation of green chemistry to meet environmental and economic goals simultaneously [22]. According to Paul Anastas and John Warner, the first to publish the 12 principles of green chemistry during the 1990s, “The main concept of Green Chemistry is the use of chemical skills and knowledge to reduce or eliminate the use or generation of hazardous substances during the planning, manufacturing and application of chemicals in order to minimize threats to the health of operators and the environment” [23].

The 12 principles of green chemistry are as follow: [24]

1. Prevent Waste.
2. Atom Economy.
3. Less hazardous synthesis.
4. Design benign chemicals.
5. Benign solvents and auxiliaries.
6. Design for energy efficiency.

7. Use of renewable feedstocks.
8. Reduce derivatives.
9. Catalysis.
10. Design for degradation.
11. Real time analysis for pollution prevention.
12. Inherently benign chemistry for accident prevention.

1.6.1 Green chemistry in the synthesis of NPs

Green synthesis of NPs aims at minimizing generated waste and implementing sustainable processes. In recent years, green processes using mild reaction conditions and non-toxic precursors have been emphasized in the development of nanotechnology for promoting environmental sustainability. There is an increased need to develop environmentally benign procedures for the synthesis of metallic nanoparticles [17]. The three main steps that should be considered during the preparation of nanoparticles from a green chemistry standpoint are the choice of the solvent/medium used for the synthesis, the choice of an environmentally benign reducing agent, and the choice of a nontoxic material for the stabilization of the nanoparticles [25]. The green synthesis of NPs represents an advance over other methods because it is simple, cost-effective, relatively reproducible, and often results in more stable materials [26].

Biological resources such as bacteria, algae fungi and plants have been used to produce low-cost, energy-efficient, and nontoxic environmentally friendly metallic nanoparticle [27]. The unique properties of the NPs synthesized by biological methods are preferred over the ones produced by physical and chemical methods [28]. Biogenic reduction of metal precursors to corresponding NPs is a clean, sustainable, and an eco-friendly method, and can be easily scaled up for mass production [29]. When using biological resources, external experimental

conditions like high energy and high pressure are not required, this will reduce the use of energy one of the most important rules of green chemistry [30]. In recent studies, applying plants and their parts is gaining extreme importance in all fields focusing on a greener environment.

1.6.2 Plant mediated synthesis of nanoparticles.

Plants are known to be an important component of different ecosystems. From the ancient times to modern days, plants serve numerous sources to mankind [31]. The most used and efficient way to synthesis nanoparticles in a green manner is the use of plant extracts. Plant extracts reduce the metal ions in a shorter time as compared to microbes. Depending on plant type and concentration of phytochemicals present in the extract, nanoparticles can be synthesized within a few minutes or hours, whereas microorganism-based methods require a longer time [32]. The major drawback of microbe-mediated nanoparticle synthesis is the constraint linked to the working environment that should be sterilized, which requires trained staff, and increases the scaling-up cost [33]. All these reasons, in addition to the easy availability of plants in nature (sustainability), make them more ideal biological resources for green synthesis. Different parts of the plants can be used for synthesis of nanoparticles: seeds, fruits, leaves and roots.

For the synthesis of zero valent iron nanoparticles and iron oxides many plant extracts can be used. Plant extracts act as low-cost reducing and stabilizing agents. Iron nanoparticle synthesis is carried out at room temperature or by simply mixing the plant extract with a metal salt solution in a fixed ratio [30]. According to many studies, the polyphenols components present in the plant extract are responsible for the reduction of iron ions whereas water soluble heterocyclic components stabilize the nanoparticles formed [34].

Polyphenols are compounds possessing one or more aromatic rings with one or more hydroxyl groups. They are broadly distributed in the plant kingdom and are the most abundant secondary metabolites of plants, with more than 8,000 phenolic structures currently known, ranging from simple molecules such as phenolic acids to highly polymerized substances such as tannins [35]. Plant polyphenols have drawn increasing attention due to their potent antioxidant properties and their marked effects in the prevention of various oxidative stress associated diseases such as cancer. Plant phenolics include phenolic acids, flavonoids, and tannins.

Flavonoids are the most abundant polyphenols. The basic flavonoid structure is the flavan nucleus, containing 15 carbon atoms arranged in three rings (C6-C3-C6), which are labeled as A, B and C. Flavonoid are themselves divided into six subgroups: flavones, flavonols, flavanols, flavanones, isoflavones, and anthocyanins, according to the oxidation state of the central C ring. Their structural variation in each subgroup is partly due to the degree and pattern of hydroxylation, methoxylation, or glycosylation [35].

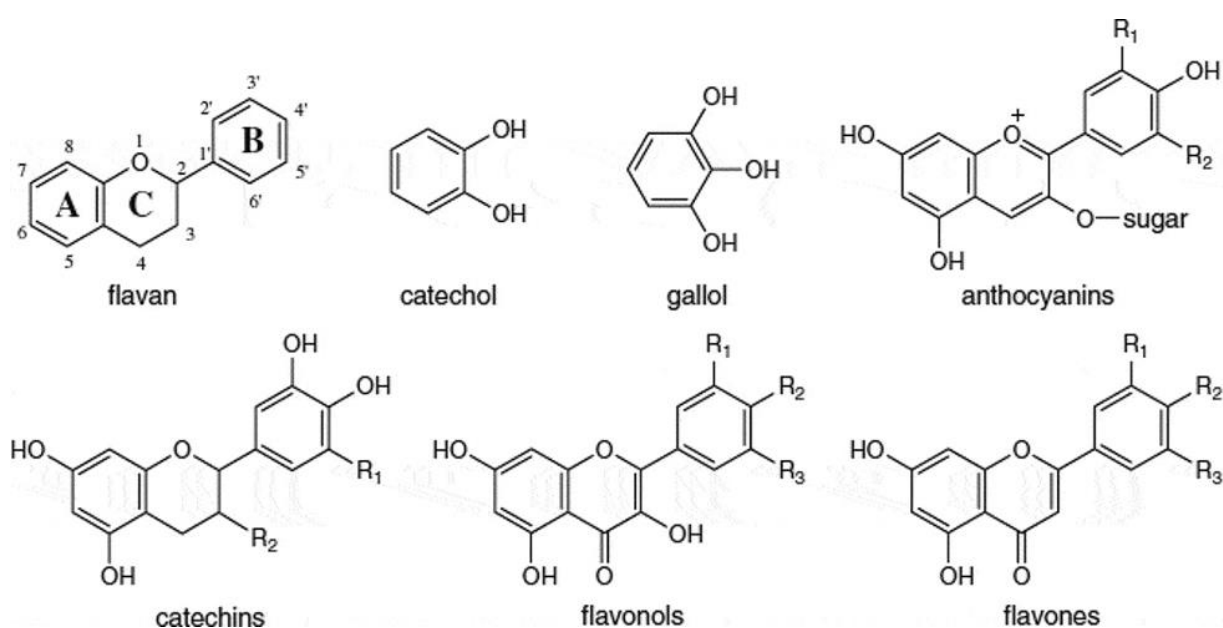


Figure 4: Flavonoids and their basic structure [36]

Phenolic acids can be divided into two classes: derivatives of benzoic acid such as gallic acid, and derivatives of cinnamic acid such as coumaric, caffeic and ferulic acid. Caffeic acid is the most abundant phenolic acid in many fruits and vegetables, most often esterified with quinic acid as in chlorogenic acid, which is the major phenolic compound in coffee. Another common phenolic acid is ferulic acid, which is present in cereals and is esterified to hemicelluloses in the cell wall [37].

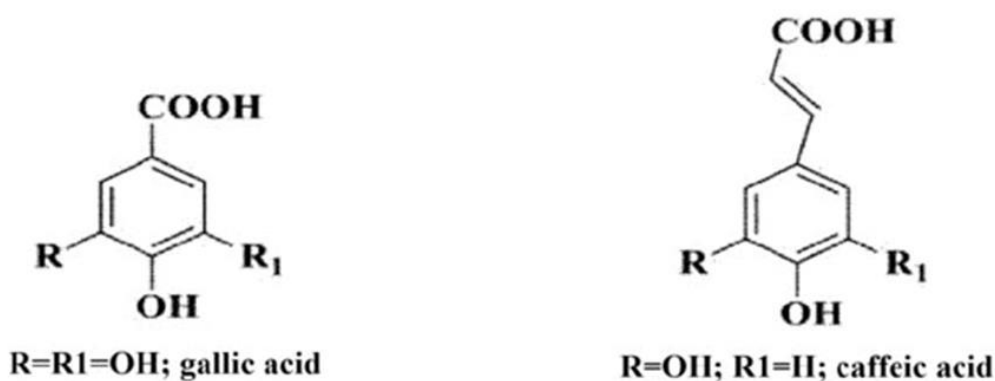


Figure 5: Phenolic acid and their structure [38]

Tannins are another major group of polyphenols in our diets and are usually subdivided into two groups: hydrolysable tannins and condensed tannins. Hydrolysable tannins are compounds containing a central core of glucose or another polyol esterified with gallic acid, also called gallotannins, or with hexahydroxydiphenic acid, also called ellagitannins. Condensed tannins are oligomers or polymers of flavan-3-ol linked through an interflavan carbon bond. They are also referred to as proanthocyanidins because they are decomposed to anthocyanidins through acid-catalyzed oxidation reaction upon heating in acidic alcohol solutions [35].

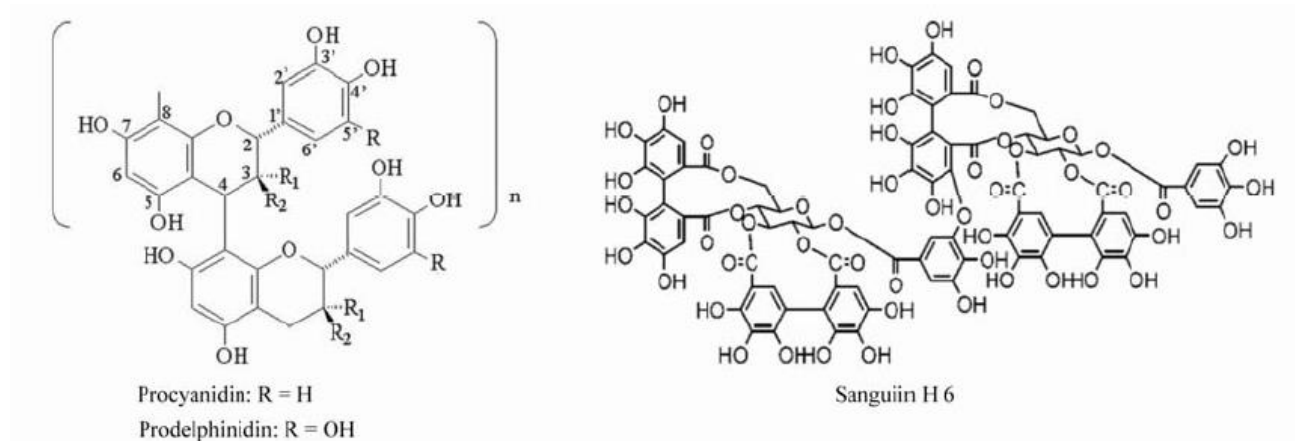


Figure 6: Tannins and their structure [35]

The synthesis of iron nanoparticles is a redox reaction where electrons will be transferred from the polyphenols to the Iron cation present in the solution taking them to a metallic form with zero charge and of nanometric scale [39]. The principal functional groups of the synthesis of NPs are alcohols, aldehydes, amines, carboxyl, ketones, hydroxyl, thiol, so that practically any biological compound that provides these groups is usable to transform metal ions into NPs [40]. However, some compounds such as tannins, flavonoids, various heterocyclic, polyphenols, reducing sugars and ascorbate are directly involved in the synthesis, while others, such as proteins, function as stabilizing agents, forming an organic coating called corona [39].

In conclusion, phytochemicals in plant extracts possess ideal redox properties that allow efficient reduction of metal precursors for conversion into their corresponding metallic nanoparticles under the influence of pH [17].

1.7 Zero-valent Iron nanoparticles

Iron is a Period 4 transition metal. It is the fourth most abundant element found in the Earth's crust [41]. It is found in minerals such as hematite and magnetite. It is a strong, ductile

and malleable metal. Its application in human history goes back about 3200 years, to the beginning of the Iron Age. Despite of this long history, the 20th century brought new application fields and challenges for metallic iron due to the emerging nanotechnology and with the production of nanosized zero-valent iron, nZVI. nZVI has markedly different properties compared to bulk iron, and it has now become one of the most important engineered nanomaterials, and the most common nanomaterial for environmental remediation such as soil and groundwater treatment due to its relatively low cost, high reactivity, and good adsorption capacity [42].

Zero-valent iron (Fe^0) is known to be an excellent electron donor, regardless of its particle size. In the presence of water Fe^0 shows a strong tendency to release electrons [43].



Iron reactivity is important in the macro scale applications especially rusting, which is an oxidation reaction of iron in the presence of water and oxygen but is a main concern at the nanoscale [41]. This extreme reactivity has traditionally made iron nanoparticles hard to study and difficult for practical applications. In order to maintain iron nanoparticles in their zero valent state, water and oxygen should be excluded, or they should be maintained in a reducing atmosphere. However, the extreme reactivity of iron nanoparticles can be beneficial in a non-oxidizing environment. Like different types of nanoparticles, iron nanoparticles have a large surface to volume ratio, thus a large portion of the atoms will be present on the surface as compared to those in the bulk materials. The large percentage of exposed atoms increases the surface activity. The large surface area and surface activity will help iron nanoparticles to be used as catalyst [44].

1.7.1 Green synthesis of ZVI NPs

Iron nanoparticles synthesized using traditional chemical approach has drawbacks including the use of toxic and very expensive chemical substances such as sodium Borohydride(NaHB_4) organic solvents, stabilizing and dispersing agents. Moreover, these materials when not stabilized have practical difficulties due to particle immobilization, agglomeration, the possible adherence to soil or organic particles and passivation effects via oxidative loss. Therefore, the development of clean, biocompatible, non-toxic and ecofriendly methods for synthesizing nanoparticles is required. Green synthesis of nanoparticles using naturally occurring reagents such as plant extracts that can act as reducing and capping agents has a potential application in nanotechnology. It is superior to other methods because it often results in more stable materials. Recently, considerable studies have been devoted to using plant extracts. [31, 44, 29] The approach is a green route and far more efficient than the traditional production method due to the decrease in agglomerate size and enhanced mobility of the particles in applications such as for ground water remediation [45].

1.7.2 Applications of ZVI NPs

Many recent studies have indicated the potential of iron nanoparticles (NPs) for environmental remediation [17, 42, 46]. Among metallic nanoparticles, iron nanoparticles have promising advantages that can combat environmental pollution. The interest in nanoscale zero-valent iron in environmental remediation is increasing due to the reactivity of nanoscale iron having a large surface area to volume ratio [17]. The production of iron nanomaterials, such as metallic iron and iron oxide via a more convenient greener route, is a great step forward in the development of nanomaterials. Several green methods have been adopted to perform the synthesis of iron NPs such as the use of biocompatible green reagents (biopolymers, ascorbic

acid & amino acids...), the synthesis by microorganisms (Bacteria, Fungi & Algae) and finally the use of plant extracts which has been proved to be the simplest, most cost effective and reproducible approach [17]. Plants produce more stable metal nanoparticles and have proved to be the best candidates for fast and large-scale synthesis as compared to microorganisms [47]. These production processes can be carried out without significant environmental pollution, thereby setting new standards in highly sustainable and economically viable clean and green technologies.

Currently, several wastewater treatment techniques are applied and the utilization of nanomaterials for pollutant removal is an emerging technology. The publications that study the effect of iron-based nanoparticles on wastewater have drastically increased [48]. In their work, T. Aragaw et al. used zero valent iron nanoparticles to remove water contaminant. Iron NPs showed a 99% removal efficiency on As(V) by absorption and Cu (II) by chemical reduction [49]. E. Murgueitio et al. evaluated the removal of total petroleum hydrocarbons (TPHs) from water and soil after treatment with zero valent iron nanoparticles. After treatment, water has showed removals of 85.94% of TPHs while the soil treated for 32 h reached a removal of 81.90% of contaminant [46].

Several recent studies have reported on the antimicrobial activity of zero valent iron nanoparticles. Some studies has found that zero valent iron nanoparticles exhibited a stronger antimicrobial activity than other iron-based nanoparticles [50]. Zero valent iron nanoparticles were proven to inhibit the growth and that the activity of *E. coli*, *Staphylococcus aureus* [51]. The cytotoxic effects appear to be associated principally with an oxidative stress. This stress can result from the generation of reactive oxygen species with the interplay of oxygen with reduced iron species or from the disturbance of the electronic and/or ionic transport chains due to the strong affinity of the nanoparticles for the cell membrane [52]. Faryal Batool et al. tested the Antimicrobial activity of FeNPs against four bacterial strains including *Klebsiella*

pneumonia, *Bacillus subtilis*, *Micrococcus leutus*, and *Escherichia coli*. FeNPs were found effective especially against *Escherichia coli* and *Klebsiella pneumonia* [53].

1.7.3 Green synthesis of iron NPs using Malva extracts

Many plants and fruits were used for the green synthesis of Iron NPs. In his work, Biruck Desalegn et al. used mango peel extract for the synthesis of Iron NPs [45]. S. Machado et al. used the extract of a mixture of 26 different tree leaves type including Apple, Apricot, Avocado, Cherry, Eucalyptus, Kiwi, Lemon and many others [54]. Walnut Green skin was also used by Asghar Hamzezadeha et al. [55]. For the first time, aqueous extract of *Malva parviflora* is used as a sustainable source of reducing and capping agents for the synthesis of zero valent iron nanoparticles. *Malva parviflora* is an annual, a biennial or a perennial herb plant that is native to Northern Africa, Europe and Asia and is widely adapted elsewhere [56]. The plant has a deep strong tap root system [57]. *Malva parviflora* has different common names such as small mallow, cheese weed (the seeds grow in a round flattened pod that is similar to a cheese wheel) and cheese weed mallow. *Malva parviflora* can grow in waste ground, roadsides, and plains. *Malva parviflora* can be found in different regions in Lebanon. It grows up to 50 cm in height [58]. The broad leaves have 5-7 lobes and are 8-10 cm in diameter. It has small white or pink flowers with 4-6 mm long petals [56]. The plant does not have a distinguished taste but does make a pleasant addition to salads and can be cooked as a green. Both the leaves and the flower are edible. The phytochemical screening of the Lebanese *Malva Parviflora* showed that both the leaves and stems of the plant contain polyphenol, flavonoid, tannin, alkaloid, resin and saponin [59]. *Malva parviflora* leaf extracts show an anti-inflammatory and antioxidant activities [58]. *Malva parviflora* grown in Lebanon shows high antioxidant activity which will make it a useful source of natural products that can be used to treat diseases associated with oxidative stress [60].

Taxonomy of Malva: [58]

1. Kingdom: Plantae
2. Division: Tracheophyta (vascular plants)
3. Class: Magnoliopsida (seed plants that produce an embryo with paired cotyledons and net-veined leaves)
4. Superorder: Rosanae (flowering plants)
5. Order: Malvales
6. Family: Malvaceae
7. Genus: Malva
8. Species: parviflora

Like other plant, Malva parviflora is rich in polyphenols and can be suitable for the plant mediated green synthesis of metal nanoparticles. It has been used before for the synthesis of silver nanoparticles [61]. Despite the use of M. parviflora in traditional medicine, very few pharmacological and phytochemical studies are reported assessing its therapeutic properties.



Figure 7: Malva Parviflora

Chapter 2- Materials and Methods

2.1 Chemical reagents

All the reagents used in this study were of analytical grade and used as received without any further purification. Ferric chloride hexahydrate $\text{FeCl}_3 \cdot 6\text{H}_2\text{O}$ (98%) was purchased from Acros Organic, sodium hydroxide (NaOH) (98.5 – 100%) from Fluka. Distilled water was used in the preparation of all solutions.

2.2 Malva extract preparation

Fresh Malva stems and leaves were collected from the Metn district in the Mount Lebanon and rinsed thoroughly with tap water followed by distilled water to remove dust and dirt. They were then air-dried for 4 days under a shade before use. The extraction was performed by boiling 5 g of washed and dried Malva into 200 ml of distilled water for 30 min followed by soaking for 1 hour. The solution was then filtered by whatman filter paper to get a clear extract and the pH was adjusted to 10 by adding a certain volume of 1 M NaOH solution. The extract was stored at 4°C for future use.

2.3 Synthesis of Zero valent iron nanoparticles

The synthesis of ZVI nanoparticles was carried out by the reduction of ferric ions with the plant extract at a ratio 2:1 under inert N_2 gas atmosphere following the process described by Z. Pan et al. [62]. Therefore, 20 mL of the Malva extract were added gradually using a burette to 10 ml of aqueous 100 mM $\text{FeCl}_3 \cdot 6\text{H}_2\text{O}$ solution under constant stirring for 1 hour at room temperature. The Malva extract was used as both reducing and stabilizing agent. The formation

of ZVI nps was evidenced by the color change of the solution and the formation of a black precipitate as indicated in Figure 10. The reaction mixture was centrifuged at 8000 rpm and the resulting black pellet was then washed three times with deionized water first and with ethanol at the end then dried overnight in a 50°C oven. Samples were stored in a sealed vial for future experiments. To determine the effect of different experimental parameters on the synthesis of ZVI nps, one experimental parameter (pH, malva soaking time, and iron precursor concentration) was changed while the others were kept constant.

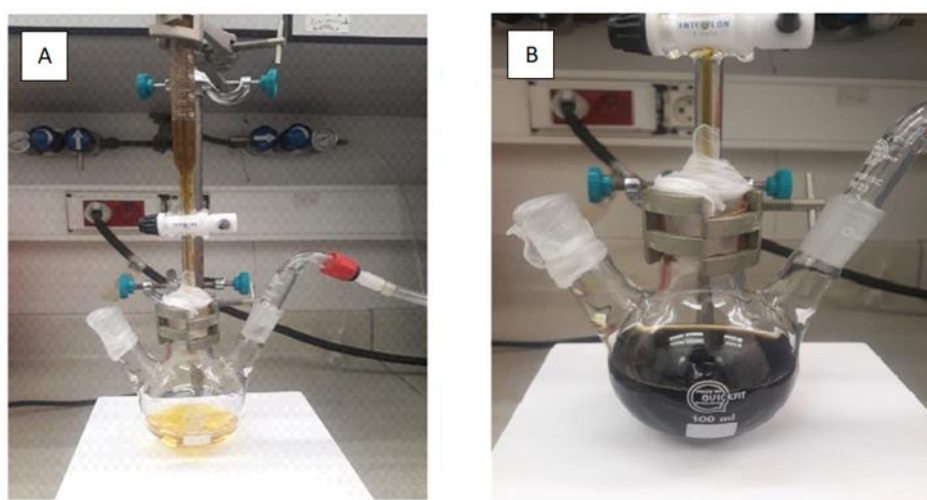


Figure 8: A- experimental setup B-black precipitate formation

2.4 Characterization of the synthesized nanoparticles

The synthesised ZVI nps were subjected to various characterisation techniques which provide specific properties such as particle size and size distribution, zeta potential, surface chemistry and crystalline structure. Malvern Zetasizer nano ZSP version 7.10 was used to analyze the NPs size and Zeta potential. FTIR- perkin Elmer UA TR two Spectrum was used to verify the main characteristics peaks of the green synthesis. In order to identify the crystalline phase of the prepared nanoparticles, X-ray diffraction (XRD) was performed using a Bruker

D4 ENDEAVOR with Cu/K- α radiation. The operating target voltage was 50 kV and the tube current was 50 mA. In the paragraphs below, the basic theory behind each technique and its various instrumentation aspects is detailed.

A. Dynamic light scattering (DLS):

Dynamic light scattering (DLS) is based on the Brownian motion of dispersed particles. When particles are dispersed in a liquid, they move randomly in all directions. The principle of Brownian motion is that particles are constantly colliding with solvent molecules. These collisions cause a certain amount of energy to be transferred, which induces particle movement. The energy transfer is more or less constant and therefore has a greater effect on smaller particles. As a result, smaller particles are moving at higher speeds than larger particles. If you know all other parameters which have an influence on particle movement, you can determine the hydrodynamic diameter by measuring the speed of the particles.

The relation between the speed of the particles and the particle size is given by the Stokes-Einstein equation. The speed of the particles is given by the translational diffusion coefficient D . Further, the equation includes the viscosity of the dispersant and the temperature because both parameters directly influence particle movement. A basic requirement for the Stokes-Einstein equation is that the movement of the particles needs to be solely based on Brownian motion. If there is sedimentation, there is no random movement, which would lead to inaccurate results. Therefore, the onset of sedimentation indicates the upper size limit for DLS measurements. In contrast, the lower size limit is defined by the signal-to-noise ratio. Small particles do not scatter much light, which leads to an insufficient measurement signal.

A single frequency laser is directed to the sample contained in a cuvette. If there are particles in the sample, the incident laser light gets scattered in all directions. The scattered light is

detected at a certain angle over time and this signal is used to determine the diffusion coefficient and the particle size by the Stokes-Einstein equation [63]:

$$dH = kT / 3\eta\pi D$$

Where dH represents the hydrodynamic diameter, k the Boltzmann's constant (1.38×10^{-23} N.m.K⁻¹), T the absolute temperature in Kelvin, η the solvent viscosity (N.s.m⁻²), and D the diffusion coefficient (m².s⁻¹).

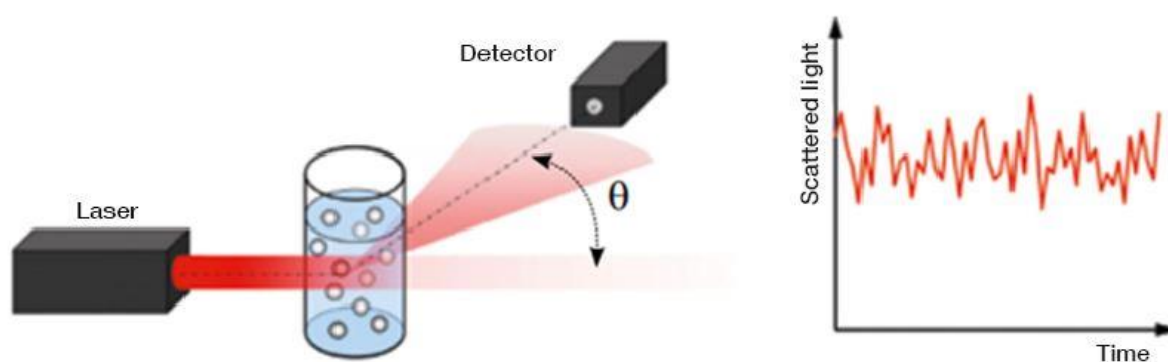


Figure 9 Basic DLS setup [64]

B. Fourier transform infrared

Fourier transform infrared spectroscopy (FTIR) is a universal analytical tool for the evaluation of a wide range of materials, especially for identification of unknown materials. It has been used to identify pure substances, mixtures, impurities, and compositions of various materials [65]. FTIR spectroscopy study the interactions between matter and electromagnetic radiation that appear in the form of a spectrum. In infrared spectroscopy, IR radiation is passed through a sample. Some of the infrared radiation is absorbed by the sample and some of it is transmitted. The radiation that is absorbed is converted by the sample to vibrational or rotational energy. Each molecule has a spectrum fingerprint that makes it unique and allows it to be distinguished from other molecules [66].

IR radiation is a group of electromagnetic waves (EMR) with wavelengths longer than visible radiation, invisible to the human eye. FTIR spectrum is recorded between 4000 and 400 cm^{-1} . A typical FTIR spectrometer includes a source of light, sample cell, detector, amplifier, A/D convertor, and a computer. Radiation from the sources reach the detector after it passes through the interferometer. The signal is amplified and converted to a digital signal by the A/D convertor and amplifier, after which the signal is transferred to the computer where the Fourier transform is carried out [67].

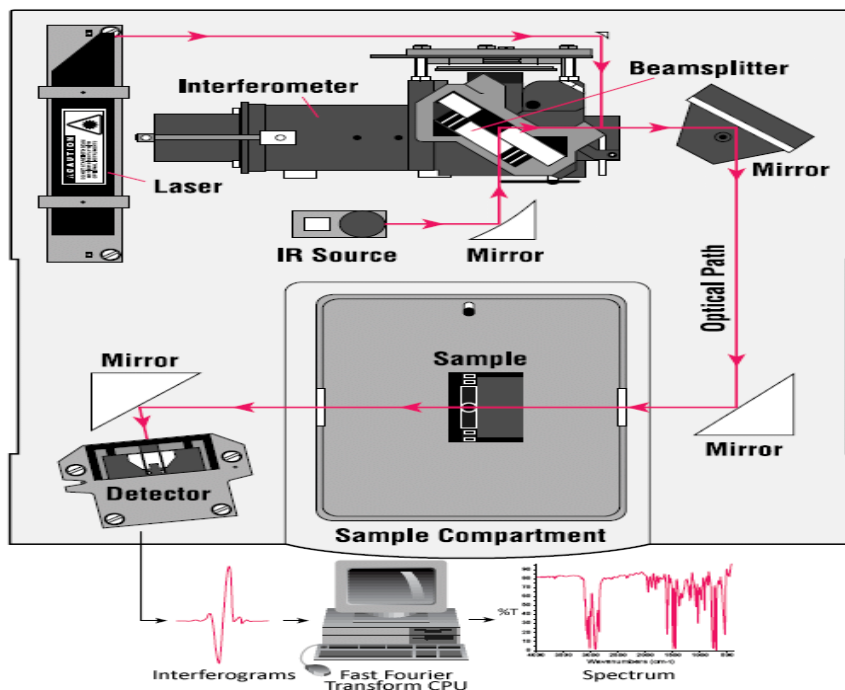


Figure 10: FTIR layout [68]

C. X-ray Diffraction (XRD):

X-ray diffraction analysis (XRD) is a technique used in materials science to determine the crystallographic structure of a material. XRD works by irradiating a material with incident X-rays and then measuring the intensities and scattering angles of the X-rays that leave the material. X-ray diffraction is based on constructive interference of monochromatic X-rays and

a crystalline sample. These X-rays are generated by a cathode ray tube, filtered to produce monochromatic radiation, collimated to concentrate, and directed toward the sample.

D. Scanning electron microscopy characterization

In this work, scanning electron microscopy (SEM) wasn't performed. Based on many studies that used SEM analysis to understand the topology of the synthesized zero valent iron nanoparticle using plant extract, it was found that green synthesized zero valent iron nanoparticles using plant extract were spherical in shape [45, 69, 70, 71]

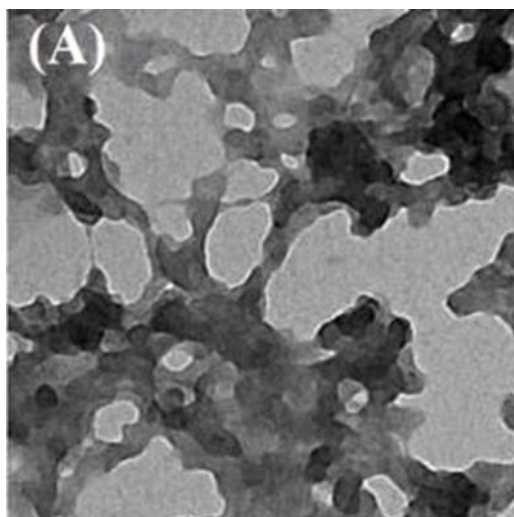


Figure 11: SEM image of green synthesized zero valent iron nanoparticles using ricinus communis seeds extract [70]

2.5 Antimicrobial properties

Human pathogenic Gram- negative *Escherichia coli* and Gram-positive *Staphylococcus aureus* bacterial strains were used for antimicrobial study of ZVI nps by disk diffusion method. The discs were soaked with distilled water, malva leave extract, FeCl_3 solution and synthesized zero valent iron nanoparticles solution. Tryptic soy agar plates, a general-purpose, nonselective

media providing enough nutrients to allow for a wide variety of microorganisms to grow were used. Agar plates were seeded with 8 hours broth culture of *S. Aureus* 3.9×10^7 Cfu/pellet and *E.coli* 4.9×10^7 Cfu/pellet . Lyophilized bacteria were used and were revived by adding 2 ml of phosphate buffer solution pH= 7.4 . Using sterilized dropping pipettes, samples were carefully added to the wells and allowed to diffuse at room temperature for 2 hours. The plates were then incubated at 37 °C for 24 hours. Then, the plates were observed to identify the presence of an inhibition zone for both microorganisms. Amoxicillin was used as positive control.

Chapter 3: Results and Discussion

The effect of some parameters such as Malva soaking time, FeCl₃ concentration and pH values were investigated for their effect on the synthesised M-ZVI nanoparticles.

3.1 Effect of Malva soaking time at different pH values on the hydrodynamic size of the synthesized M-ZVI nanoparticles

The ideal extraction method should be cost-effective, simple, less time-consuming, and carried out easily in any laboratory. After boiling for 30 minutes, Malva leaves were soaked for an additional time (30 min, 1 hour and 2 hours) to improve extraction. The resulting solution is acidic with a pH value of 2.5. The pH is adjusted to different values using a 1 M solution of NaOH. Table 2 displays the effect of Malva soaking at different time intervals and different pH values on the hydrodynamic size of the synthesized M-ZVI nanoparticles.

pH	Soaking time		
	30 min	1 h	2 h
2.5	3200	1751	2898
4	1773	1231	2800
6	520	185	142
7	241.5	135	147
8.5	288	134	100
9.3	290	101	110
10	258.8	102	86

Table 2: FeNPs size variation at different pH with different malva soaking time

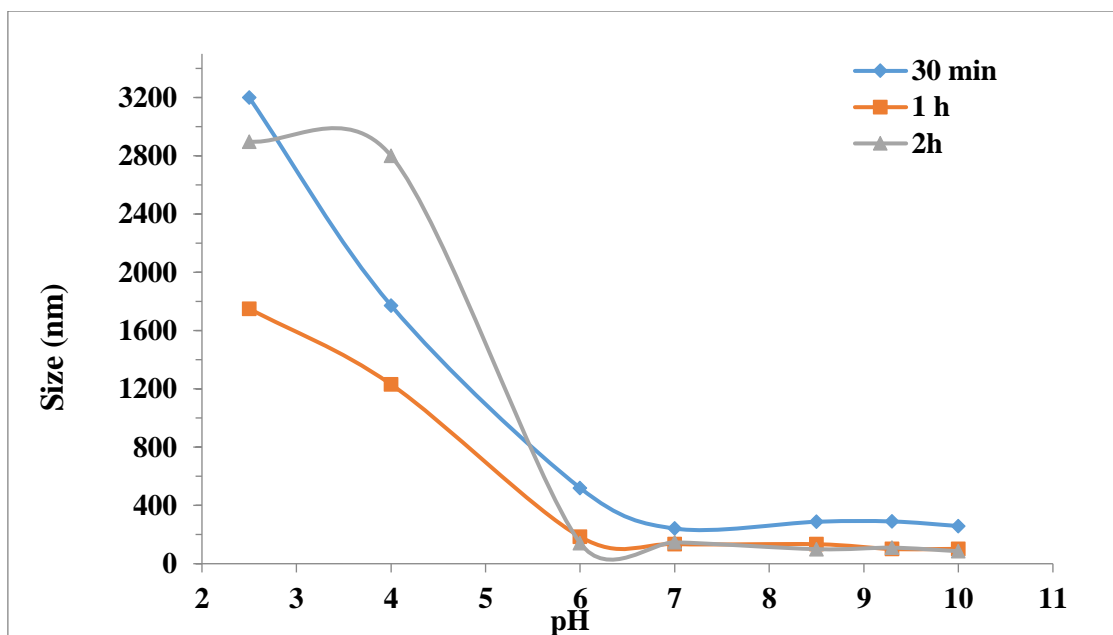


Figure 12: FeNPs size variation as a function of pH for different malva soaking time

As shown in Figure 11, the hydrodynamic size of the M-ZVI nanoparticles decreases with increasing pH values. The hydrodynamic size decrease subtly from pH 2 to pH 6 as the zeta potential of the particle at lower pH values is low which enhance the particles aggregation and thus increase the hydrodynamic size of the particles. The size change for pHs above 7 is minimal as high values of zeta potential between -19 and -23.5 Mv were already reached at pH 7 which enhance the particles stability. The same pattern in size change as a function of pH is observed for the 3 different soaking time. the best results at neutral pH are obtained with malva extract soaked for 1 hour and since the particles are designed to be tried for antimicrobial activities the desired pH will be 7. In addition to the application, soaking malva for 1 hour only will be less time consuming since similar results are obtained when malva is soaked for 2 hours as shown in Figure 11. In fact, Chandini et al. concluded that extraction times higher than 60 min can degrade the flavins and affect the extraction of catechins [72]. In his study, Machado et al. considered the most favorable extraction time for different types of leave and results are

summarized in the table below. Extraction times ranged between 20 min for cherry and lemon tree leave and 80 min for pear tree [54].

Leaf	Extraction time (min)
Apricot tree	40
Cherry tree	20
Kiwi bush	20
Lemon tree	20
Mandarin tree	20
Medlar tree	20
Mulberry bush	60
Oak	20
Olive tree	40
Orange tree	20
Passion fruit bush	20
Peach tree	20
Pear tree	80
Pine tree	20
Plum tree	20
Pomegranate tree	60
Quince tree	20
Eucalyptus	40
Raspberry bush	20
Apple-tree	20
Strawberry bush	20
Black tea	20
Green tea	20
Vine	80
Avocado	40
Walnut tree	20

Table 3: Most favorable extraction time for studied leaves

3.2 Effect of FeCl₃ concentration on the hydrodynamic size of the synthesized M-ZVI nanoparticles

The effect of the iron precursor FeCl₃ on the hydrodynamic size of the synthesized particles was studied at 3 different solution concentrations 50 mM, 100 mM and 150 mM. The volume ratio of FeCl₃ solution and malva extract used in the 3 experiments is 1:2 . Figure 12 shows nanoparticle hydrodynamic size distribution as a function of the pH for the 3 different solution. We notice that for the desired pH=7 the best size was generated with the 100 mM FeCl₃ Solution. Similar results were obtained with Seyedeh-Masoumeh Taghizadeh et al. where more increase in the iron precursor has shown negative effect on the formation of nanoparticles after reaching certain concentration [73]. Raziye Kheshtzar et al. also generated better results with 50 mM FeCl₃ solution compared to the 75 mM FeCl₃ solution [74].

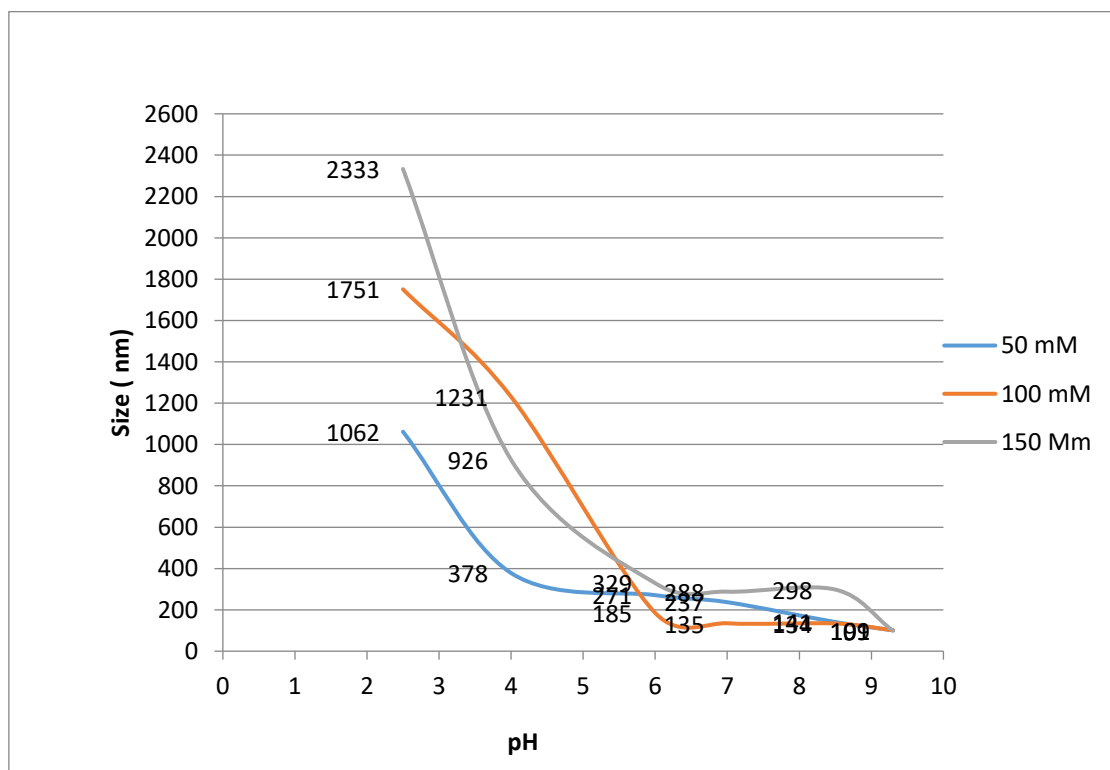


Figure 13: size variation of FeNPs with pH for 3 different FeCl₃ solution concentrations.

3.3 Effect of pH on the hydrodynamic size and zeta potential of the synthesized M-ZVI nanoparticles.

After mixing is done the pH of the synthesized solution decrease to an acidic pH = 2.5. Similar shift was observed with Monalisa Pattanayak et al. who synthesized zero valent iron nanoparticles from the Leaf Extract of *Azadirachta indica* [75]. The pH of the resulting solution was adjusted with a solution of 1 M NaOH and using a DLS – Zetasizer the size, polydispersity index and zeta potential were measured at different pHs. Polydispersity index (PdI) is used to estimate the average uniformity of a particle solution, and larger PdI values correspond to a larger size distribution in the particle sample. PdI can also indicate nanoparticle aggregation along with the consistency and efficiency of particle surface modifications throughout the particle sample. A sample is considered monodisperse when the PdI value is less than 0.2 [76]. Generated results are summarized in the table 4 .Better size and dispersion results were generated at higher pH where the particles can be considered as nearly monodispersed and not aggregated since the PDI is around 0.25. The average particle size is around 130 nm, a good size for green synthesized and coated nanoparticles since no additional capping is required for stabilization. When using chemical routes to synthesize zero valent iron nanoparticles, coating materials should be added to avoid aggregation of the particles. Stabilization of nanoparticles using coating materials rely on combined electrosteric stabilization of nZVI. Electrostatic repulsion is achieved by increasing the surface charge to increase the repulsive forces between particles, whereas steric stabilization is obtained by the adsorption of long-chain organic molecules, which hinders particle attraction [77].

pH	Size (nm)	PDI	Zeta Average (mV)
2.5	1751	1	26.93
4	1231	1	-4.42
6	185	0.5	-18.2
7	135	0.4	-19.4
8.5	134	0.24	-20.9
9.3	101	0.25	-22.07
10	102	0.25	-23.5

Table 4: FeNPs size, PDI and zeta potential variation as a function of pH

The electrostatic properties of nZVI in aqueous suspensions are controlled by the pH of the suspension, with minimum nZVI stability occurring when pH approaches the point of zero charge [78]. The point of zero charge specifies the conditions of the solution in particular, the pH value for which the surface density of positive charges equals that of negative charges. It is often regarded as a characteristic parameter for a given surface in a given aqueous solution [79].

The zeta potential is a criterion for measuring the magnitude of electrostatic repulsion or attraction between particles in a liquid suspension. It is one of the main parameters for characterizing the stability of nanoparticles in an aqueous environment [80]. The capping biomolecules existing on the surface of the FeNPs largely consist of negatively charged groups and are also responsible for greater stability of the extract mediated FeNPs. It is observed that the value of the zeta potential is more positive at more acidic pH due to dissociation of some H^+ and total protonation of the carboxyl groups, and at higher pH values there is an increase of OH^- ions in the dissociated solution and deprotonation of the carboxyl groups of gives a more negative zeta potential [81]. Biologic coatings from various plants can provide different zeta potentials ranging from -35 mV for green tea to about zero for *Hordeum vulgare*, and $+71$ mV for *Amaranthus spinosus* [82, 83]. This variation is mainly due to different

phytochemicals in various plants. Generally, the surface charge values above -30 mV are considered to be sufficient for suppressing particles agglomeration and providing a stable colloidal system [84].

3.4 FTIR Characterization

Figure 13 shows the FTIR spectrum of the Malva extract and the synthesized M-ZVI nanoparticles. FTIR analysis was conducted to determine the chemical components which were responsible for stabilizing and capping of ZVI nps. The two intense and sharp peaks at about 640 cm^{-1} and 450 cm^{-1} characteristics of the Fe-O bonds in iron oxide nanoparticles are not present in the FTIR spectrum of the synthesized nps [44]. This proves that the prepared particles are zero valent iron nanoparticles. The broad peak at around 3400 cm^{-1} is assigned for O-H stretching vibration such as phenols and/or carboxylic acids. The existence of phenolic compounds in plant extracts is important because these compounds are most often cited as being directly responsible for Fe^{3+} to Fe^0 reduction and the formation of a cladding layer on the surface of Fe NPs [62]. In the peak intensity at 3400 cm^{-1} was slightly reduced for the FeNPs after the reaction which indicated that polyphenolic substances in the malva extract were involved in the production of Fe NPs. The sharp adsorption peaks at 2850 and 2900 cm^{-1} are attributed to the symmetrical vibration of $-\text{CH}_2$ and asymmetrical vibration of $-\text{CH}_3$, respectively. The symmetric and asymmetric bending vibrations of $-\text{CH}_3$ and $-\text{CH}_2$ are further confirmed by the presence of peaks around 1400 and 1300 cm^{-1} , respectively. The influential band at 1620 cm^{-1} is due to the stretching vibration of $-\text{C}=\text{O}$ in aldehyde, ketone a carboxylic acid. However, as shown in figure 13, the absorption at band 1620 decreased and slightly shifted which could correspond to of $-\text{C}=\text{O}$ stretching of amides from aldehyde and ketones indicating that these organic compounds may be responsible for capping. The decrease in the intensity of the band for the amides could possibly demonstrate the structural change following

interaction with iron particles. The sharp peaks observed at 1020 cm^{-1} were attributed to the bending vibration of $-\text{OH}$ and stretching vibration of $-\text{C}-\text{O}-\text{C}-$ in the lignin structure of the material [85]. The FTIR of the malva extract and that of the nZVI exhibit approximately similar spectral pattern. However, the reduced intensity of the synthesized FeNPs could be due to the reduction of hydroxyl groups and the formation of iron-phenol complex [86]. Moreover, the organic capping from the Malva extract seems to protect the M-ZVI nps from oxidation. Similar results were generated with Biruck Desalegn et al. who used mango peel for the synthesis of iron nanoparticles [45]. Furthermore, J. Jeyasundari et al. generated similar FTIR spectrum for both the plant extract and the synthesized zero valent iron nanoparticles accompanied by a slight shift and intensity reduction, suggesting that biological molecules could possibly perform the dual function of formation and stabilization of FeNPs in the aqueous medium [34].

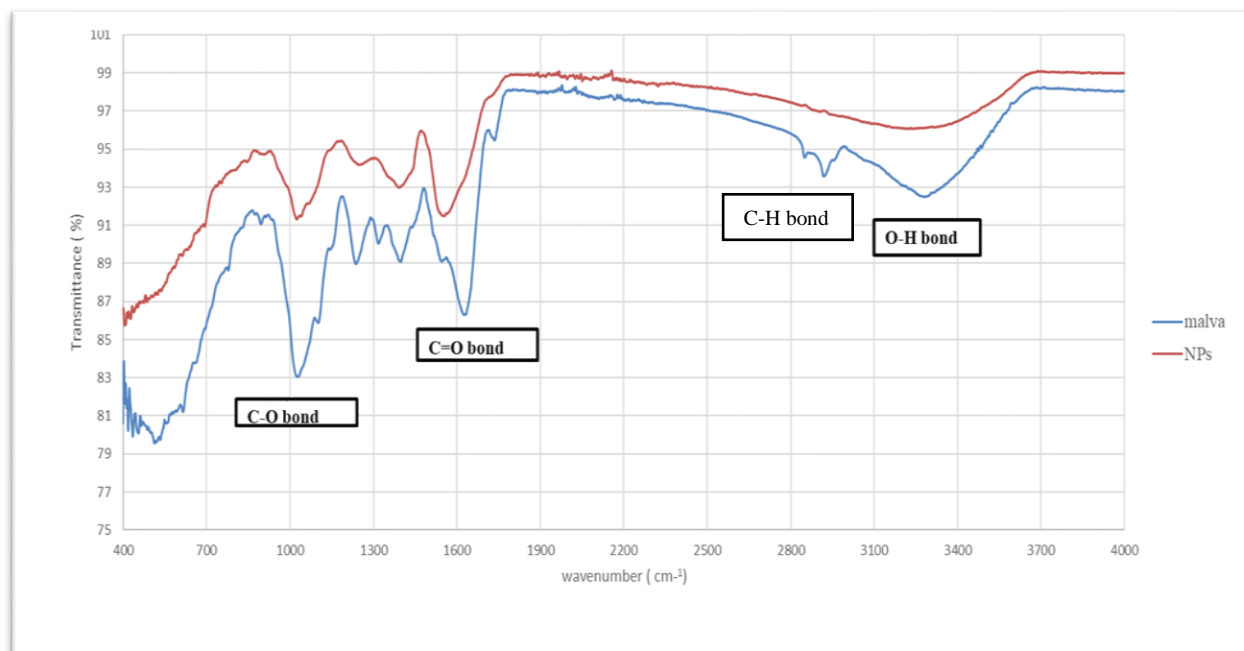


Figure 14: FTIR spectrum of malva and synthesized zero valent iron nanoparticles

3.5 XRD characterization

The XRD spectrum of the synthesized ZVI nanoparticles presented in Figure 14 shows no obvious characteristic peaks confirming the absence of any ordered crystalline structure. According to the literature, green synthesized zero valent iron nanoparticles doesn't show any specific peak unlike the XRD pattern of iron oxide nanoparticles which display different distinct peaks evidencing a crystalline structure. Fabrication of amorphous zero-valent INPs was also reported by using leaf extract of different plants such as eucalyptus, mulberry, pomegranate, and cherry [87]. The broad peak showing at $2\theta = 15^\circ$ was proposed to be due to the presence of organic component from the malva extract which are responsible for capping and stabilizing synthesized nanoparticles [74].

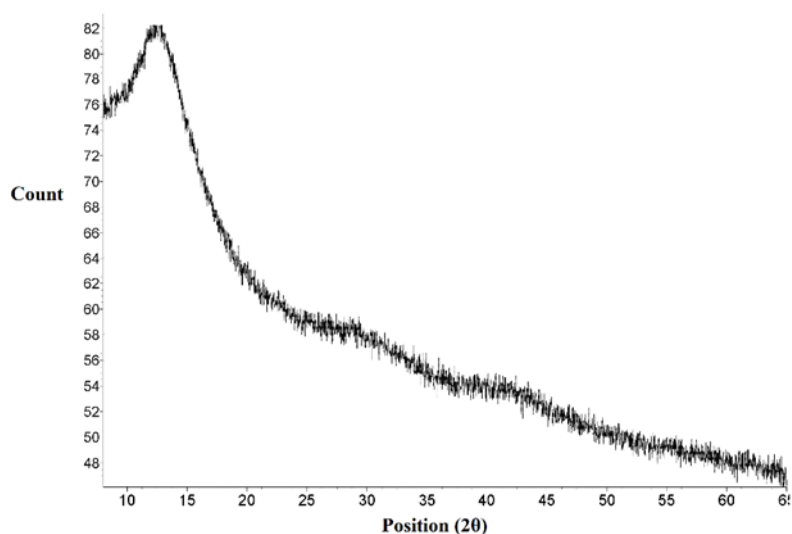


Figure 15: X-ray powder diffraction pattern of the synthesized zero valent iron nanoparticles

Similar spectrum was also obtained by Seyedeh-Masoumeh Taghizadeh et al. who was trying to find the optimal parameters for the green synthesis of zero valent iron nanoparticles [73].

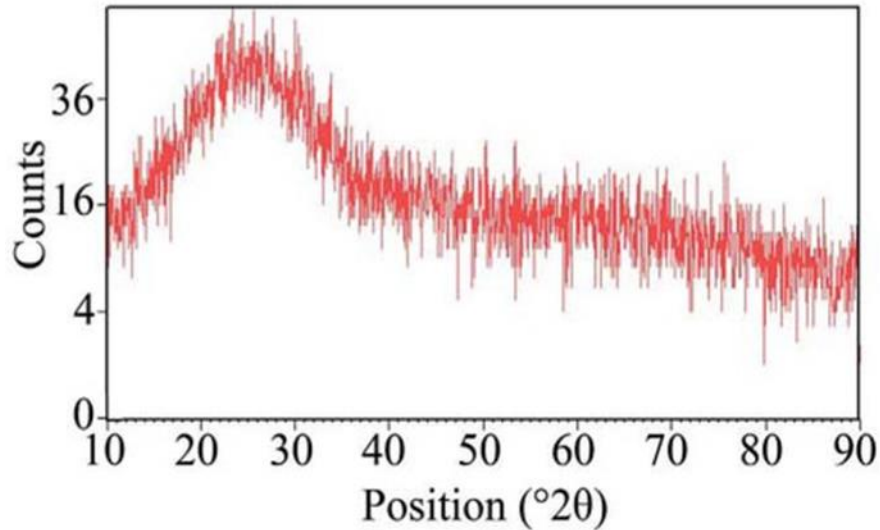


Figure 16: XRD spectrum of green synthesized FeNPs from leaves of *U. dioica* [73]

3.7 Antimicrobial activity

The anti-bacterial activity of the synthesized particles was performed on human pathogenic Gram- negative *Escherichia coli* and Gram-positive *Staphylococcus aureus*. Gram positive bacteria have a thick peptidoglycan layer and no outer lipid membrane whilst Gram negative bacteria have a thin peptidoglycan layer and have an outer lipid membrane [88]. Synthesized FeNPs were found effective against the gram-positive *Staphylococcus aureus* and inactive against *E. coli*. Lee et al. reported that FeNPs were toxic to gram-negative *E. coli* ATCC8739 in 2 mM carbonate buffer at pH 8.0 in the absence of oxygen [89]. However, under aerobic conditions, FeNPs were found not effective, no inhibition zone was observed around the disk soaked in FeNPs after 24 h. This finding suggested that FeNPs might exert significant antimicrobial effect only under anaerobic conditions. This is not the case for *staphylococcus aureus* where an inhibition zone was detected for both malva extract and FeNPs. Similar results were generated with Yi-Huang Hsueh et al. where zero valent iron nanoparticles were found to

be effective against gram positive Bacillus strains and defenseless against gram-negative Escherichia coli strains [90].

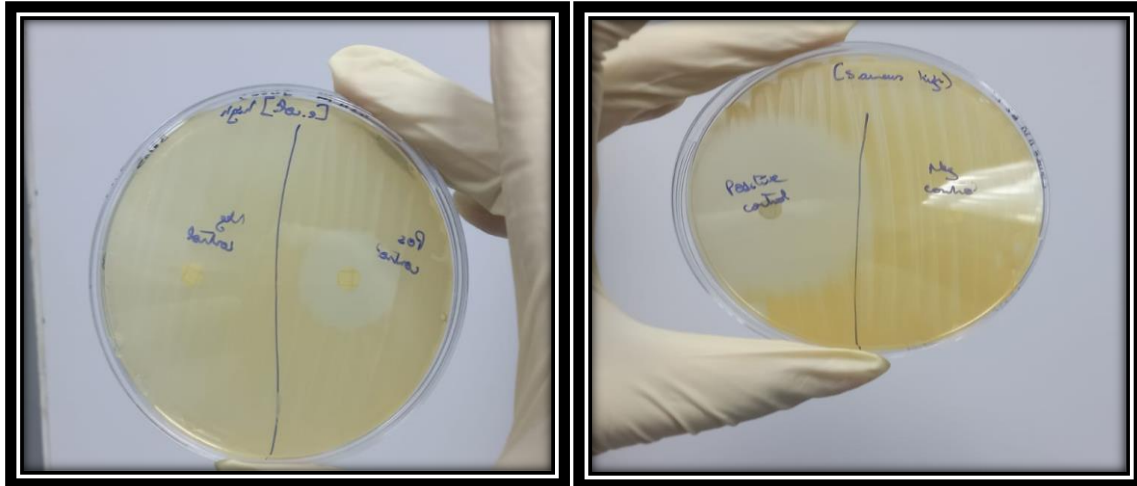


Figure 17: Positive control on E. coli and S. aureus

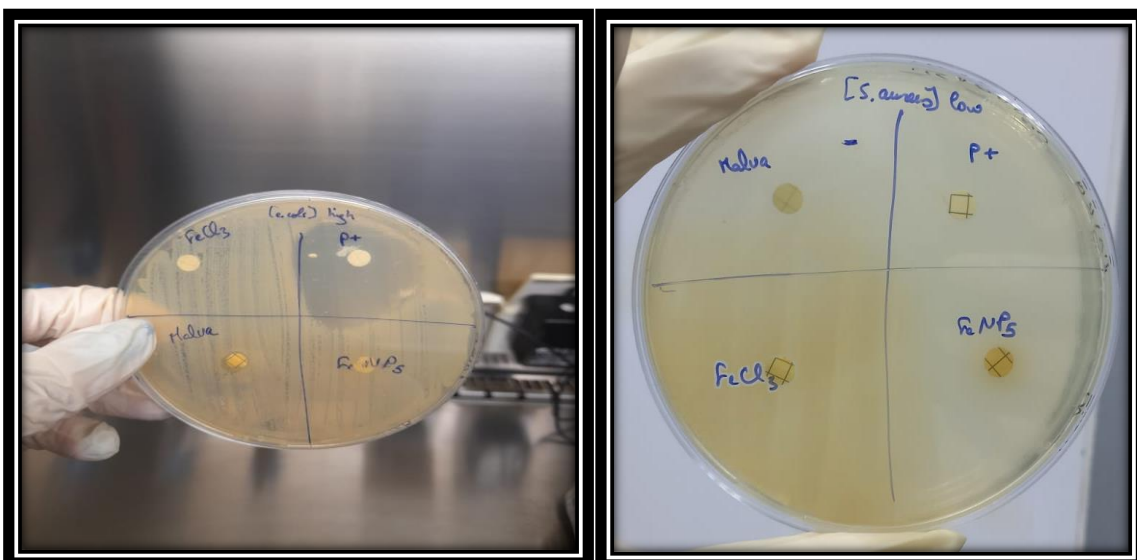


Figure 18: antibacterial activity of malva extract, FeCl₃ and FeNPs on E. coli and S. aureus

3.7 Conclusion

In this work, zero valent iron nanoparticles were successfully green synthesized for the first time from *Malva parviflora* extract which act as reducing and capping agent at the same time due to its polyphenol content. The pH of the resulting solution affected the size of the particles since there is a relation between the pH and the zeta potential of particles. More negative zeta potential was achieved at higher pHs which prevent the aggregation of the synthesized particles. Zero valent iron nanoparticles have an average size of 100 nm and are considered monodispersed. The antibacterial activity of these particles was tested on *Staphylococcus aureus* and *Escherichia coli* strains. Particles were effective against gram positive *Staphylococcus aureus*. Few studies have looked at the persisting challenges of such use and evaluated the biological interactions of zero valent iron nanoparticles. The present findings may provide a basic approach to elucidate the effects of green synthesized zerovalent iron nanoparticles toxicity on gram-positive and gram-negative bacteria specially that the number of Antibiotic resistant bacteria is increasing due to the misuse of antibiotics.

References

- [1] Samer Bayda , Muhammad Adeel, Tiziano Tuccinardi , Marco Cordani Flavio Rizzolioto Nanomedicine, "The History of Nanoscience and Nanotechnology: From Chemical–Physical Applications to Nanomedicine," *MOLECULES*, vol. 25, no. 1, 2020.
- [2] P. Y. a. V. M. Veer Singh, "Recent advances of classification, properties, synthesis and characterization of nanomaterials," *Research gate*, 2020.
- [3] S. Bhatia, *Natural Polymer Drug Delivery Systems*, Springer, 2016.
- [4] H. Mehlhorn, *Nanoparticles in the Fight Against Parasites*, Springer, 2016.
- [5] R. A. B. J. W. a. A. J. S. C. G. Granqvist, "Far-Infrared Absorption in Ultrafine Al Particles," *Physical review letters* , vol. 37, no. 625, 1976.
- [6] J. Kreuter, "Nanoparticles: a historical perspective," *International Journal of Pharmaceutics*, vol. 331, pp. 1-10, 2007.
- [7] Ibrahim Khan, Khalid Saeed, Idrees Khan , "Nanoparticles: Properties, applications and toxicity," *Arabian journal of Chemistry*, vol. 12, no. 7, pp. 908-931, 2019.
- [8] J. Y. P. M. P. D. T. a. J. C. N. Wolfgang Sigmund, "Processing and Structure Relationships in Electrospinning of Ceramic Fiber Systems," *Journal of the american ceramic society*, vol. 89, no. 2, pp. 395-407, 2006.
- [9] M. W. F. A. M. Shouheng Sunc, "Monodisperse FePt Nanoparticles and Ferromagnetic FePt Nanocrystal Superlattices," *Science*, vol. 287, no. 5460, pp. 1989-1992, 2000.
- [10] A. J. a. S. s. Manoj K. Rawat, "Studies on Binary Lipid matrix based solid lipid nanoparticles of repaglinide: in Vitro and in Vivo Evaluation," *Journal of pharmaceutical sciences* , vol. 100, no. 6, pp. 2366-2378, 2011.
- [11] S. Hassan, "A review on Nanoparticles: Their synthesis and type," *Research journal of recent sciences*, vol. 4, 2015.
- [12] Harish Kumar K, Nagasamy Venkatesh*, Himangshu Bhowmik and Anuttam Kuila, "metallic nanoparticles : a review," *Biomedical journal of scientific & ttechnical research* , vol. 2, no. 4, 2018.
- [13] Eleonora Petryayeva, Ulrich J. Krull, "Localized surface plasmon resonance: Nanostructures, bioassays and biosensing - A review," *Analytica chimica acta*, vol. 706, no. 1, pp. 8-24, 2011 .
- [14] Katherine A. Willets and Richard P. Van Duyne, "Localized Surface Plasmon Resonance Spectroscopy and Sensing," *Annual review of physical chemistry*, vol. 58, pp. 267-297, 007.
- [15] S. P. a. V. V. Burungale, *Nanomedicines for Breast Cancer Theranostics*, Elsevier, 2020.
- [16] J. S. a. X. Gao, "Nanoparticle counting: towards accurate determination of the molar concentration," *Chemical Society reviews*, vol. 43, no. 21, pp. 7267-7278, 2014.
- [17] Sadia Saif , Arifa Tahir and Yongsheng Chen, "Green Synthesis of Iron Nanoparticles and Their Environmental Applications and Implications," *Nanomaterials*, vol. 6, no. 11, p. 209, 2016.

- [18] Jagpreet Singh, Tanushree Dutta, Ki-Hyun Kim, Mohit Rawat, Pallabi Samddar and Pawan Kumar, "Green' synthesis of metals and their oxide nanoparticles: applications for environmental remediation," *Journal of Nanobiotechnology*, vol. 84, 2018.
- [19] R. a. M. d. P. GorkaSalas, "Synthesis of Inorganic Nanoparticles," *Frontiers of Nanoscience*, vol. 4, pp. 35-79, 2012.
- [20] R. V. a. A. G. Ramakrishna Matte, "Recent progress in the synthesis of inorganic nanoparticles," *Dalton transaction* , vol. 41, no. 5089, 2012.
- [21] Seiichi Hisano and Kazuhisa Saito, "Research and development of metal powder for magnetic recording," *Journal of Magnetism and Magnetic Materials*, vol. 190, no. 3, pp. 371-381, 1998.
- [22] Pietro Tundo, Paul Anastas, David StC. Black, Joseph Breen, Terrence Collins, Sofia Memoli, Junshi Miyamoto, Martyn Polyakoff, and William Tumas, "Synthetic pathways and processes in green Chemistry," *Pure and applied chemistry*, vol. 72, no. 7, p. 1207–1228, 2000.
- [23] Bianca Aparecida de Marco, Bárbara Saú Rechelo, Eliane Gandolpho Tótolí, Ana Carolina Kogawa, Hérida Regina and Nunes Salgado, "Evolution of green chemistry and its multidimensional impacts: A review," *Saudi Pharmaceutical Journal*, vol. 27, pp. 1-8, 2019.
- [24] Mohd Wahid, Faizan Ahmad, Nafees Ahmad, "Green Chemistry: Principle and its Application," in *2nd International Conference on Advancement in Engineering, Applied Science and Management*, New Delhi, 2017.
- [25] Poovathinthodiyil Raveendran, Jie Fu, and Scott L. Wallen, "Completely “Green” Synthesis and Stabilization of Metal Nanoparticles," *Journal of the American Chemical Society*, vol. 125, pp. 13940-13941, 2003.
- [26] D. F. S. S. S. K. T. a. G. E. J. P. Monaliben Shah, "Green Synthesis of Metallic Nanoparticles via Biological Entities," *Materials* , vol. 8, pp. 7278-7308, 2015.
- [27] Kaushik N. Thakkar, MS*, Snehit S. Mhatre, MS, Rasesh Y. Parikh, MS, "Biological synthesis of metallic nanoparticles," *Nanomedicine*, 2009.
- [28] Imtiyaz Hussain. Ajey Singh, Himani Singh, "Green synthesis of nanoparticles and its potential application," *Biotechnology letters* , no. 38, pp. 545-560, 2016.
- [29] Amit Kumar Mittal Yusuf Chisti Uttam Chand Banerjee, "Synthesis of metallic nanoparticles using plant extracts," *Biotechnology advances*, vol. 31, no. 2, pp. 346-356, 2013.
- [30] Mihir Herlekar, Siddhivinayak Barve, and Rakesh Kumar, "Plant-Mediated Green Synthesis of Iron Nanoparticles," *Journal of Nanoparticles*, 2014.
- [31] A.A.Haleemkhan, Naseem and B.Vidya Vardhini, "Synthesis of Nanoparticles from Plant Extracts," *International Journal of Modern Chemistry and Applied Science*, vol. 2, no. 3, pp. 195-203, 2015.
- [32] Mahendra Rai and Alka yadav, "CRC 675—current trends in phytosynthesis of metal nanoparticles," *Biotechnology*, vol. 28, no. 4, p. 277–284, 2008.
- [33] Muthuswamy Sathishkumar , Krishnamurthy Sneha and Yeoung-Sang Yun, "Immobilization of silver nanoparticles synthesized using Curcuma longa tuber powder and extract on cotton cloth for bactericidal activity," *Bioresource Technology*, vol. 101, no. 20, p. 7958–7965, 2010.
- [34] J. Jeyasundari1*, P. Shanmuga Praba, Y. Brightson Arul Jacob, V. S. Vasantha and V. Shanmugaiah, "Green Synthesis and Characterization of Zero Valent Iron Nanoparticles

- from the Leaf Extract of Psidium Guajava Plant and Their Antibacterial activity," *Chemical Science Review and Letters*, vol. 6, no. 22, pp. 1244-1252, 2017.
- [35] Jin Dai and Russell J. Mumper, "Plant Phenolics: Extraction, Analysis and Their Antioxidant and Anticancer Properties," *Molecules*, vol. 15, pp. 7313-7352, 2010.
- [36] Munawar Abbas, Farhan Saeed, Faqir Muhammad Anjum, Muhammad Afzaal, Tabussam Tufail, Muhammad Shakeel Bashir, Adnan Ishtiaq, Shahzad Hussain & Hafiz Ansar Rasul Suleria, "Natural polyphenols: An overview," *International Journal of Food Properties*, vol. 20, no. 8, pp. 1689-1699, 2017.
- [37] Massimo D'Archivio, Carmela Filesi, Roberta Di Benedetto, Raffaella Gargiulo, Claudio Giovannini and Roberta Masella, "Polyphenols, dietary sources and bioavailability," *Annali dell'Istituto superiore di sanita*, vol. 43, no. 4, pp. 348-361, 2007.
- [38] Roxana BANC, Carmen SOCACIU, Doina MIERE, Lorena FILIP, Anamaria COZMA, Oana STANCIU and Felicia LOGHIN, "Benefits of Wine Polyphenols on Human Health: A Review," *Bulletin of University of Agricultural Sciences and Veterinary Medicine Cluj-Napoca Food Science and Technology*, vol. 71, no. 2, pp. 79-87, 2014.
- [39] M. F. ., M. C. a. C. C. Yosmery Vitta, "Synthesis of iron nanoparticles from aqueous extract of Eucalyptus robusta Sm and evaluation of antioxidant and antimicrobial activity," *Materials Science for Energy Technologies*, vol. 3, p. 97-103, 2020.
- [40] A. Y. a. A. G. Mahendra Rai, "Current Trends in Phytosynthesis of Metal Nanoparticles," *Critical reviews in biotechnology*, vol. 28, no. 4, pp. 277-284, 2008.
- [41] D. L. Huber, "nanoparticles Synthesis, Properties, and Applications of Iron Nanoparticles," *Small*, vol. 1, no. 5, pp. 483-499, 2005.
- [42] M. K. Tibor Pasinszki, "Synthesis and Application of Zero-Valent Iron nanoparticles in water treatment environmental remediation, catalysis, and their biological effect," *Nanomaterials*, vol. 10, no. 917, 2020.
- [43] Wei-xian Zhang and Daniel W. Elliott, "Applications of Iron Nanoparticles for Ground water Remediation," *Remediation journal*, vol. 16, no. 2, pp. 7-29, 2006.
- [44] Alireza Ebrahiminezhad, Alireza Zare-Hoseinabadi, Aydin Berenjian and Younes Ghasemi, "Green synthesis and characterization of zero valent iron nanoparticles using stinging nettle (*Urtica dioica*) leaf extract," *Green process synthesis*, vol. 6, p. 469-475, 2017.
- [45] M. Z. a. R. BiruckDesalegn, "Green synthesis of zero valent iron nanoparticle using mango peel extract and surface characterization using XPS and GC-MS," *Heliyon*, vol. 5, no. 5, 2019.
- [46] L. C. M. A. A. I. A. D. a. a. O. T. Erika Murgueitio, "Green Synthesis of Iron Nanoparticles: Application on the Removal of Petroleum Oil from Contaminated Water and Soils," *Journal of Nanotechnology*, 2018.
- [47] V. L. P. L. L. M. N. R. P. S. M. M. C. L. M. A. D. S. J. S. a. S. K. B. Ratul Kumar Das, "Biological synthesis of metallic nanoparticles: plants, animals and microbial aspects," *Nanotechnology for Environmental Engineering*, 2017.
- [48] F. M. B. a. B. A. A. Assefa Aragawa, "Iron-based nanoparticles in wastewater treatment: A review on synthesis methods, applications, and removal mechanisms," *Journal of Saudi Chemical Society*, 2021.
- [49] R. C. S. a. S. B. S. Praveen K. Tandon, "Removal of Arsenic(III) from Water with Clay-Supported Zerovalent Iron Nanoparticles Synthesized with the Help of Tea

- Liquor," *Industrial & Engineering Chemistry Research*, vol. 52, pp. 10052-10058, 2013.
- [50] Q. R. a. P. K. S.A. Mahdy, "Antimicrobial activity of zero-valent iron nanoparticles," *International Journal of Modern Engineering Research*, vol. 2, pp. 578-581, 2012.
- [51] Q. J. R. a. P. K. Saba A.Mahdy, "Antimicrobial Activity of zero-valent Iron Nanoparticles," *International Journal of Modern Engineering Research*, vol. 2, no. 1, pp. 578-581, 2012.
- [52] W. A. J. R. M.-A. R. C. C. D. T. W. A. M. J. C. W. M. R. W. a. J.-Y. B. Mélanie Auffan 1, "Relation between the redox state of iron-based nanoparticles and their cytotoxicity toward *Escherichia coli*," *Environmental science and technology*, vol. 581, no. 17, pp. 6730-6735, 2008.
- [53] M. S. I. S. K. J. K. B. a. M. I. Q. Faryal Batool, "Biologically synthesized iron nanoparticles (FeNPs) from *Phoenix dactylifera* have anti-bacterial activities," *Scientific reports*, vol. 11, 2021.
- [54] S. J. H. J. a. C.-M. S.Machado, "Green production of zero-valent iron nanoparticles using tree leaf extracts," *Science of The Total Environment*, vol. 445, pp. 1-8, 2013.
- [55] M. F. K. R. a. Y. P. Asghar Hamzezadeha, "A novel green synthesis of zero valent iron nanoparticles (nZVI) using walnut green skin: characterisation, catalytic degradation and toxicity studies," *International Journal of Environmental Analytical Chemistry*, 2021.
- [56] S. S. a. P. B. Vellingiri Vadivel, "Distribution of flavonoids among Malvaceae family members – A review," *International journal of green pharmacy*, vol. 10, no. 1, 2016.
- [57] O. A. a. M. S. A.J. Afolayan, "Total Phenolic Content and Free Radical Scavenging Activity of *Malva parviflora* L. (Malvaceae)," *Journal of biological sciences*, vol. 8, no. 5, pp. 945-949, 2008.
- [58] N. Ajeet Singh, "Ethnomedicinal, Antimicrobial and Pharmacological aspects of *Malva parviflora* Linn.: A review," *The Journal of Phytopharmacology*, vol. 6, no. 4, pp. 247-250, 2017.
- [59] HUSSEIN FARHAN, HASSAN RAMMAL, AKRAM HIJAZI, BASSAM BADRAN, "PRELIMINARY PHYTOCHEMICAL SCREENING AND EXTRACTION OF POLYPHENOL FROM STEMS AND LEAVES OF A LEBANESE PLANT *MALVA PARVIFLORA* L.," *International Journal of Current Pharmaceutical Research*, vol. 4, no. 1, pp. 55-59, 2012.
- [60] H FARHAN, H RAMMAL, A HIJAZI, H HAMAD, A DAHER, M REDA, B BADRAN, "IN VITRO ANTIOXIDANT ACTIVITY OF ETHANOLIC AND AQUEOUS EXTRACTS FROM CRUDE *MALVA PARVIFLORA* L. GROWN IN LEBANON," *Asian Journal of Pharmaceutical and Clinical Research*, vol. 5, no. 3, pp. 234-238, 2012.
- [61] W. H. E. a. A. S. Mervat F. Zayed, "Malva parviflora extract assisted green synthesis of silver nanoparticles," *Spectrochimica Acta Part A: Molecular and Biomolecular Spectroscopy*, vol. 98, p. 423-428, 2012.
- [62] Y. L. B. S. G. O. a. Z. C. Zibin Pan, "Green synthesis of iron nanoparticles using red peanut skin extract: Synthesis mechanism, characterization and effect of conditions on chromium removal," *Journal of Colloid and Interface Sciences*, vol. 558, pp. 106-114, 2020.
- [63] S. F. a. C. Betzel, *Radiation in bioanalysis: Dynamic Light Scattering (DLS)*, Springer, 2019.

- [64] F. Babick, "Chapter 3.2.1 - Dynamic light scattering (DLS)," in *Characterization of Nanoparticles*, Elsevier, 2019, pp. 137-172.
- [65] D. K. a. M. Pitucha, "Application of FTIR Method for the Assessment of Immobilization of Active Substances in the Matrix of Biomedical Materials," *Materials*, vol. 12, 2019.
- [66] D. P. V. H. C. S. O. C. a. G. M. Ahmed Fadlelmoula, "Fourier Transform Infrared (FTIR) Spectroscopy to Analyse Human Blood over the Last 20 Years: A Review towards Lab-on-a-Chip Devices," *Micromachines*, vol. 13, no. 187, 2022.
- [67] A. K. S. a. S. Irvani, *Green Synthesis, Characterization and Applications of Nanoparticles*, Elsevier, 2019.
- [68] R. Al-Oweini, *Polyoxometalates Immobilized onto Mesoporous Organically-Modified Silica Aerogels for Selective Oxidation Catalysis of Anthracene*, Beirut: Researchgate , 2009.
- [69] D. A. a. P. Y. S. K. Sravanthi, "Green synthesis, characterization of biomaterial-supported zero-valent iron nanoparticles for contaminated water treatment," *Journal of Analytical Science and Technology*, 2018.
- [70] M. F. A. S. E. a. M. E. E.-K. Ahmed M. Abdelfatah, "reen Synthesis of Nano-Zero-Valent Iron Using Ricinus Communis Seeds Extract: Characterization and Application in the Treatment of Methylene Blue-Polluted Water," *ACS Omega*, vol. 6, no. 39, pp. 25397-25411, 2021.
- [71] N. S. a. S. N. P. R. Kumar, "Potential of green synthesized zero-valent iron nanoparticles for remediation of lead-contaminated water," *International Journal of enviromental sciences and technology* , vol. 12, pp. 3943-3950, 2015.
- [72] L. J. R. ., M. K. G. ., D. J. H. a. R. S. S K Chandini, "Enzymatic treatment to improve the quality of black tea extracts," *Food chemistry*, vol. 127, no. 3, 2011.
- [73] A. Z.-H. A. B. Y. G. a. A. E. Seyedeh-Masoumeh Taghizadeh, "Effective Parameters in the Green Synthesis of Zero-valent Iron Nanoparticles as a Fenton-like Catalyst," *Journal of Environmental Treatment Techniques*, vol. 8, no. 1, pp. 442-447, 2020.
- [74] A. B. S.-M. T. Y. G. A. G. A. a. A. E. Raziye Kheshtzar, "Optimization of reaction parameters for the green synthesis of zero valent iron nanoparticles using pine tree needles," *Green Process Synthesis* , vol. 8, p. 846–855, 2019.
- [75] M. P. a. P. Nayak, "Green Synthesis and Characterization of Zero Valent Iron Nanoparticles from the Leaf Extract of Azadirachta indica (Neem)," *World Journal of Nano Science & Technology*, vol. 2, no. 1, pp. 6-9, 2013.
- [76] J. W. S. S. T. W. a. T. L. K.-U. Katherine N. Clayton, "Physical characterization of nanoparticle size and surface modification using particle scattering diffusometry," *Biomicrofluids* , vol. 10, no. 5, 2016.
- [77] M. A. A. S. A.-F. a. A. M. A.-T. Hesham M. Ibrahim, "Stability and Dynamic Aggregation of Bare and Stabilized Zero-Valent Iron Nanoparticles under Variable Solution Chemistry," *Nanomaterials*, vol. 10, no. 2, 2020.
- [78] B. G. Y. W. V. L. M. R. M. C. Q. H. a. L. Y. Yuan Tian, "Deposition and transport of functionalized carbon nanotubes in water-saturated sand columns," *Journal of hazardous materials*, vol. 213, pp. 265-272, 2012.
- [79] C. C. a. D. C.Rey, "Metallic, Ceramic and Polymeric Biomaterials," *Comprehensive Biomaterials*, vol. 1, pp. 187-221, 2011.

- [80] M. A. E. a. P. B. Shahram Eslami, "Green synthesis of safe zero valent iron nanoparticles by *Myrtus communis* leaf extract as an effective agent for reducing excessive iron in iron-overloaded mice, a thalassemia model," *RSC advances*, no. 8, pp. 26144-26155, 2018.
- [81] E. R. D. P. S. F. J. L. F. J. P. L. a. M. A. S. Leiriana Aparecida Pinto Gontijo, "pH effect on the synthesis of different size silver nanoparticles evaluated by DLS and their size-dependent antimicrobial activity," *Materia*, vol. 25, no. 4, 2020.
- [82] M. S. L. A. S. O. D. A. Y. I. T. M. K. N. Makarov VV, "Biosynthesis of stable iron oxide nanoparticles in aqueous extracts of *Hordeum vulgare* and *Rumex acetosa* plants," *Langmuir*, vol. 30, pp. 5982-5988, 2014.
- [83] H. M. a. M. Matheswaran, "Amaranthus spinosus Leaf Extract Mediated FeO Nanoparticles: Physicochemical Traits, Photocatalytic and Antioxidant Activity," *ACS Sustainable Chem. Eng.*, vol. 3, pp. 3149-3156, 2015.
- [84] G. G. C. J. L. D. M. S. E. & R. J. M. Wallace, "Nanostructured carbon electrodes," *Journal of materials chemistry*, vol. 20, pp. 3553-3562, 2010.
- [85] S. R. ., J. S. R. R. K. S. L. J.-S. C. a. d. J. R. K. Naincy Sahu, "Process optimization and modeling of Methylene Blue adsorption Using Zero-Valent Iron Nanoparticles synthesized from Sweet Lime Pulp," *Applied sciences* , vol. 9, 2019.
- [86] P. U. R. a. P. Rajasekharreddy, "Green synthesis of silver-protein (core-shell) nanoparticles using Piper betle L. leaf extract and its ecotoxicological studies on *Daphnia magna*," *Science Direct* , vol. 389, no. 1, pp. 188-194, 2011.
- [87] J. G. P. ., H. P. A. N. ., J. T. A. a. C. D.-M. S Machado, "Characterization of green zero-valent iron nanoparticles produced with tree leaf extracts," *Sci Total Environ.*, vol. 533, pp. 76-81, 2015.
- [88] K. Steward, "Gram Positive vs Gram Negative," *Technology networks*, 2019.
- [89] J. Y. K. W. I. L. K. L. N. J. Y. a. D. L. S. Changha Lee, "Bactericidal Effect of Zero-Valent Iron Nanoparticles on *Escherichia coli*," *Environmental science & technology*, vol. 42, pp. 4927-4933, 2008.
- [90] P.-H. T. K.-S. L. a. W.-J. K. Yi-Huang Hsueh, "Antimicrobial effects of zero-valent iron nanoparticles on gram-positive *Bacillus* strains and gram-negative *Escherichia coli* strains," *Journal of nanobiotechnology*, vol. 15, no. 1, pp. 77-88, 2017.
- [91] A. B. Y. S. C. A. D. a. M. K. D. Jaison Jeevanandam, "Review on nanoparticles and nanostructured materials: history, sources, toxicity and regulations," *Beilstein Journal of Nanotechnology*, vol. 9, pp. 1050-1074, 2018.
- [92]